J. Mat. NanoSci. 2019, 6(2), 47-66 Review

Journal of
Materials NanoScience

Critical evaluation of pharmaceutical rational design of Nano-Delivery systems for Doxorubicin in Cancer therapy

Bhupender S. Chhikara,[1,*] Brijesh Rathi,[2] and Keykavous Parang[3,*]

[1]Department of Chemistry, Aditi Mahavidyalaya, University of Delhi, Bawana, Delhi-110039. India. [2]Laboratory for Translational Chemistry and Drug Discovery, Department of Chemistry, Hansraj College, University of Delhi, Delhi-110007. India. [3]Center For Targeted Drug Delivery, Department of Biomedical and Pharmaceutical Sciences, Chapman University School of Pharmacy, Harry and Diane Rinker Health Science Campus, Irvine, California 92618, United States.

Submitted on: 16-June-2019, Accepted on: 24-July-2019, Published on: 2-Sept-2019

ABSTRACT

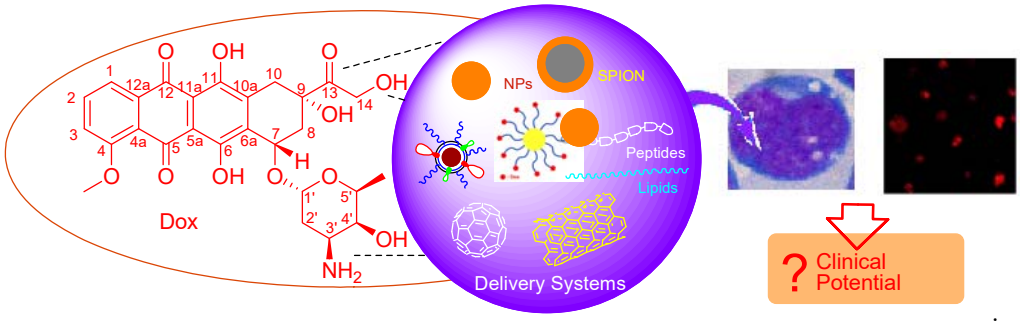

Doxorubicin (Dox), an antineoplastic drug, has been extensively used for the treatment of different cancers. Dox is hydrophilic and therefore distributes to normal organs at a faster rate. Due to its required high doses, it poses severe toxicity, such as cardiotoxicity and nephrotoxicity. Diverse approaches, including nanoparticulate delivery systems, have been designed and evaluated to improve its delivery to the target site and reduce toxicity to normal organs; however, this has met little success. Here in this review, we have discussed various systems (metal nanoparticles, carbon nanotubes, fullerenes, liposomes, dendrimers, cyclic peptides, and other covalent/non-covalent systems) that have been used for Dox. We have critically evaluated their designing and outcome (*in vitro* and *in vivo*) with potential applications in the clinical setting.

Keywords: Adriamycin, Cancer Drug, CPP, Drug Delivery System, Lipophilic Dox, TAT peptide

INTRODUCTION

Doxorubicin (Dox) **1** (Figure 1) alias Adriamycin is an anthracycline-based anti-cancer molecule. It is obtained biosynthetically from fungus wild type strains of *Streptomyces* and *Streptomyces peucetius*. It is a bright red colored powder in physical appearance. Structurally, it has an anthracycline core substituted at different positions. There is a methoxy group in position 4. Positions 5 and 12 have quinoid functionality. Positions 6 and 11 of the third ring have hydroxyl groups. The fourth saturated ring is disubstituted with hydroxyl and (2-hydroxyacetyl) group at 9 position and has an aminohydroxyoxirane ring attached through ethereal linkage at position 7 (Figure 1). In overall, Dox has 1 amino, 3 oxy, 5 hydroxyl, and 3 carbonyl moieties; which makes it highly hydrophilic and that is why it is readily soluble in water.

Dox acts on fast-growing cells and as an antitumor antibiotic. It is commonly used as an anticancer agent for the treatment of leukemia, breast carcinoma, and other solid tumors. Dox has also been used for the treatment of other tumors like ovarian carcinoma, liver cancer, and stomach cancer; however, nowadays,

*Corresponding Authors: Prof. K. Parang and Dr. B.S. Chhikara
Email: parang@chapman.edu (KP), drbs@aditi.du.ac.in (BS),
Tel: +1 (714) 516-5489 (KP), +91-9818811510 (BS),
Fax: +1 (714) 516-5481 (KP)

Cite as: *J. Mat. NanoSci., 2019, 6(2), 47-66.*
urn:nbn:sciencein.jmns.2019v6.95

 ISSN 2394-0867
http://pubs.thesciencein.org/jmns

it is not the first choice in the clinic for these cancers due to the emergence of drug resistance.[1,2] In cellular assays, Dox does not show high antiproliferative activity against ovarian carcinoma cells SK-OV-3, showing an IC_{50} value of 5 μM following 48 h of incubation.[3] Dox is given to patients through intravenous injections and generally used in combination chemotherapy along with other anticancer agents, however, it is used as a general reference standard in anticancer cellular (*in vitro*) assay for evaluation of new drug molecules.[4–6]

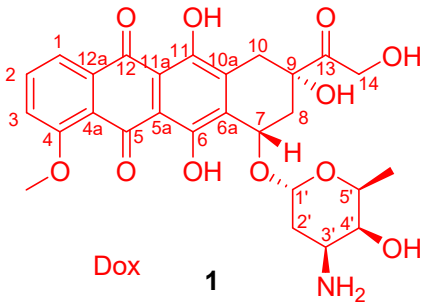

Figure 1. Chemical Structure of Dox **1**.

Dox has a high volume of biodistribution, and also its short physiological half-life leads to its rapid distribution, fast excretion, and ultimately low bioavailability of the drug at target sites. Furthermore, Dox has a high rate of efflux and is actively extruded from cancer cells overexpressing P-glycoprotein (PgP).[7] Thus, high cumulative doses of Dox are required in cancer chemotherapy to achieve optimum therapeutic effect. However, the higher doses lead to dose-dependent side effects, such as cumulative cardiotoxicity, nephrotoxicity, and extravasation, which compromises its clinical applications.[8] The most dangerous side effect of Dox is cardiomyopathy, leading to congestive heart failure. The rate of cardiomyopathy is dependent on its cumulative dose, with an incidence of about 4% when the dose of Dox is 500–550 mg/m², 18% when the dose is 551–600 mg/m², and 36% when the dose exceeds 600 mg/m².[9] There are several ways in which Dox is believed to cause cardiomyopathy, including oxidative stress, downregulation of genes for contractile proteins, and p53 mediated apoptosis.[9] The drug dexrazoxane is used to mitigate cardiotoxicity caused by Dox. Other common adverse effects of Dox include hair loss (seen in most of those treated with the drug), myelosuppression (a compromised ability of the body's bone marrow to produce new blood cells), nausea and vomiting (which are seen in roughly 30-90% of people treated with the drug), oral mucositis, oesophagitis, diarrhoea, skin reactions (including hand-foot syndrome), and localized swelling and redness along the vein in which the drug is delivered.

A number of different pharmacological methods and delivery systems have been evaluated to reduce side effects caused by administration of Dox. The strategies include the utilization of enhanced permeability and accumulation properties of various delivery systems. The inclusion of Dox in delivery system could be done either by physical entrapment i.e. non-covalent entrapping or by chemical bond formation between Dox and Delivery vehicle i.e. covalent entrapping. The non-covalent entrapping has been done using liposomes while the covalent modification is required for nanoparticular systems. In the delivery systems, the pegylated liposomes that encapsulate Dox are available as Doxil.[10] Doxil was initially developed for the treatment of Kaposi's sarcoma, which is an AIDS-related cancer[11] of the skin (symptoms include lesions under the skin, in the lining of mouth, nose, throat or other organs). The pegylated liposomes facilitate the accumulation of the drug in epidermal skin while this also leads to side effect commonly called as hand-foot syndrome. This occurs as the drug leaks from capillaries to palm and soles resulting in redness and peeling of skin from hands and palms. This limits the use of Doxil over free Dox.[12] However, Doxil is less cardiotoxic, an advantage over free Dox.[13]

The other substitutions for efficient Dox application have also been explored.[14] Several metal nanoparticles and carbon nanosystems have the potential to deliver the drug at the target organ with reduced side effects. Dox has been evaluated with nanoparticles by covalent conjugation with Gold, Silver, Iron, CdS, fullerenes and other nanoparticles.[15] This review is meant to analyze the methodology adopted for conjugation of Dox with various metal nanoparticles and their outcomes with potential applicability in clinical settings.

2. METALLIC NANOPARTICLES

Nanosized particles of different metals (viz. gold, iron, silver, quantum dots, etc.) have been employed for drug delivery due to enhanced permeability by nanoparticles.[16] The drug loading involves either **non-covalent** direct adsorption on a metal surface or a **covalent** attachment to the nanoparticle through covalently bonded linkers.[17]

Both strategies have been adopted for the delivery of Dox by using different nanoparticles. The non-covalent systems incorporated Dox by entrapment in outer shells of the nanoparticles. The examples of non-covalent systems designs for iron and/or gold nanoparticles included[18] (1) *Adsorption of Dox on nanocarrier surfaces*, such as free Dox adsorbed inside hollow structures of PEG 5000 over (Au) nanoparticles,[19] Dox complexed with ferrous Fe^{2+} over gold nanoparticles,[20] and Dox intercalated in the RNA aptamer,[21] (2) *Affinity of Dox towards coating materials*, such as diffusion in coating polymers e.g. PAMAM copolymer (Iron Oxide NP),[22] PAsp-g-C18 copolymer (Iron Oxide NP),[23] carboxymethylchitosan, and entrapment in coating materials such as entrapment inside PEO-TMA-FA polymer-coated gold nanoparticles, HSA-Dopamine (Iron Oxide NP),[24] Pluronic polymer (Iron Oxide NP),[25] and PTMC-b-PGA copolymer.[14]

The covalently linking of Dox to metallic nanoparticles has been achieved by disulfide linkage, hydrazone linkage, amide, carbamate and ester bonds. In most cases, a second layer of polymer (PEG, Chitosan, etc.) is introduced over the surface of the metal nanoparticles, the functional group over polymer or organic compounds layer is further used for covalent coupling with Dox. The type of bonding or point of attachment between Dox and nanoparticles play important role in the efficient utilization of anti-cancer properties of Dox and delivery properties of nanoparticles system as discussed in following sections.

2.1. Gold Nanoparticles (Au-NPs)

The gold nanoparticles (Au-NPs) constitute one of prominent systems that have been extensively studied for the delivery of various drugs. The rich chemistry of gold nanoparticles synthesis[26] and subsequent application in synthetic chemistry, drug delivery, materials development and other fields puts these NPs on frontline for evaluation for delivery of different drugs including Dox. Dox has been attached via different type of covalent bonding with layer of organic or polymer molecules coated over the Au-NPs.

2.1.1 Linking Through Disulfide Bonds

Dox has been covalently attached through disulfide linkage (-S-S-) for the possible release of Dox by thiol reducing enzymes aided by acidic pH inside the lysosomes.[27] The study by Gu et al. coated the Au-NPs with amine functionalized polyethylene glycol (PEG-NH_2).[28] The surface amine groups were functionalized to incorporate terminal thiol groups on the polymer (making PEG-SH), which was used for coupling with the thiol-modified Dox to generate the Dox bound to the end of PEG-SH via disulfide bonds (Au-PEG-S-S-Dox) (Figure 2). Dox was located over the surface of the Au-NPs, i.e. on the terminal ends of PEG coating. The group reported the estimated concentration of 70 µM of Dox/240 µM of Au in Au-PEG-SS-Dox nanoparticles, i.e. 0.3 µM of Dox/µM of Au.

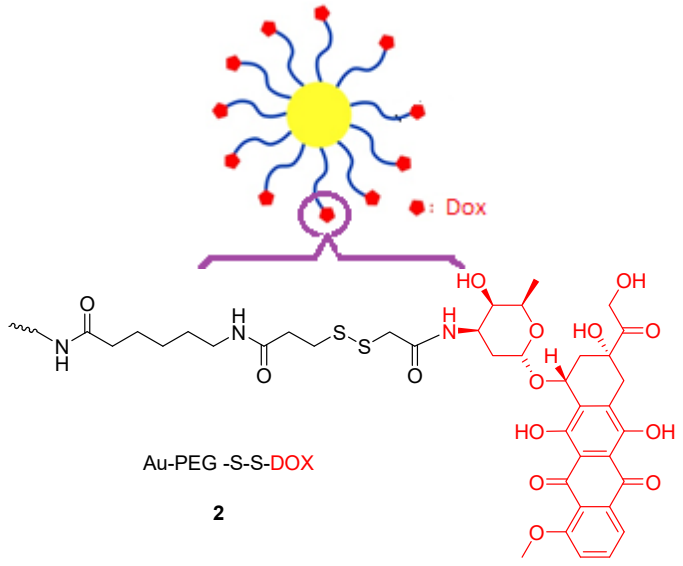

Figure 2. Structure of Au-PEG-SS-DOX conjugate as represented by Gu et al[28].

The intracellular uptake of Au-PEG-SS-DOX was greater than that of free Dox in the Multi-Drug Resistant (MDR) cells as observed by confocal images, however, the drug conjugate concentration required for increased level of drug accumulation in MDR cells was at doses greater than 15 µM, which is a much higher concentration compared to parent drug Dox. The cytotoxicity of Au-PEG-SS-DOX nanoconjugates system was in proportion to drug accumulation as released Dox concentration enhanced its cytotoxicity against MDR cancer cells. This report by Gu et. al. discussed the Dox linking via the disulfide bond to Au-NPs, however, the amine group of Dox was utilized in attachment and amide bond is the first bond with Dox in the reported conjugate (figure 2); the disulfide being the part of linker. This bonding pattern would have bearing on the end pharmacological parameters analyzed.

2.1.2. Hydrazone Bonds

The carbonyl group of Dox has been used for the conjugation with polymer layer coated Au-NPs. Prabaharan et al. developed Au-NPs coated with an amphiphilic block copolymer having hydrazine amine groups.[29] Dox was conjugated via hydrazone linkage onto the hydrophobic inner shell of Au-nanoparticle-copolymer system. As linkage takes place in the inner layer of this system, Dox has to cross outer PEG shell to reach to hydrazine groups for conjugation that is placed in hydrophobic poly(L-aspartate) PLA layer (Figure 3). For sufficient loading, the diffusion and reaction required 24 h of contact between Dox and Au-NP copolymer system and further 48 h of dialysis to remove unreacted Dox. Dox loading obtained on this system by this procedure was 17% w/w. The folic acid was attached on the outer PEG layer for target specific delivery of conjugate (figure 3).

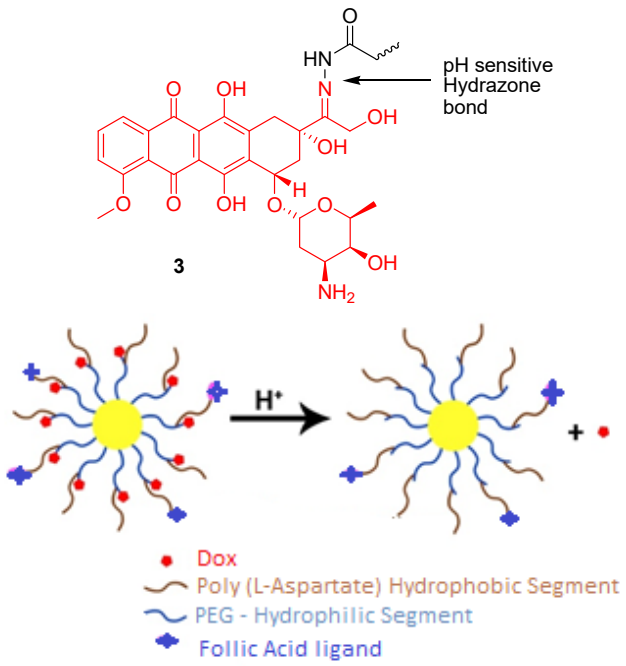

Figure 3. The structure of Au-P(LA-Dox)-b-PEG-OH/FA conjugate and pH-dependent release of Dox as reported by Prabaharanet al.[29]

The release of Dox from this Au-NP-Poly-Dox system was strongly pH dependent; further influenced by the structure of the nanoparticle system. At pH 7.4, only 10% of Dox was released from Au-NP-Poly-Dox system after 3 days. At lower pH, the release was more near to completion. At pH 5.3 and 6.6, Dox released from Au-NP-Poly-Dox system was 94% and 83%, respectively, after 45h. This release is more suited to *in vivo* conditions for keeping Dox intact to Au-NP-Poly-Dox system during transportation and circulation in the blood and releasing

Dox inside the tumor cells as pH is lower there. The confocal images indicated more total cellular uptake in 4T1 cells for Dox compared to Au-NP-Poly-Dox, and also the free Dox localized inside the nucleus rapidly while the Au-NP-Poly-Dox localized in the cytoplasm and released Dox in the nucleus as expected.

Aryal et al. reported attachment of Dox using Dox-hydrazine functionalized with thiol group for attachment of Au-NPs surface.[30] The Au-NPs were stabilized with thiol functionalized PEG (Figure 4). This way, both Dox and PEG were attached to Au-NP using thiol group. The Au-NPs were stabilized by thiolated methoxy polyethylene glycol (MPEG-SH) and methyl thioglycolate (MTG) at an equal molar ratio. Anticancer drug Dox was conjugated to the MTG segments of the thiol-stabilized Au-NPs using hydrazine as the linker. The resulting hydrazone bonds formed between Dox molecules and the MTG segments of the thiol-stabilized Au-NPs are acid cleavable, thereby providing a strong pH-responsive drug release profile. The MPEG segments attached to the Au-NPs provide the Au NPs with excellent solubility and stability in an aqueous medium while potentially enhancing the circulation time. Dox loading level was determined to be 23 wt.%. The dox release rate from the DOX conjugated Au-NPs in an acid medium (*i.e.*, pH 5.3) was higher than that in physiological conditions (*i.e.*, pH 7.4). The Dox-conjugated Au-NPs and/or Dox released from them were found both at the perinuclear regions, and the nuclei of 4T1 tumor cells after incubation with the Dox conjugated Au-NPs solution for 28 h.

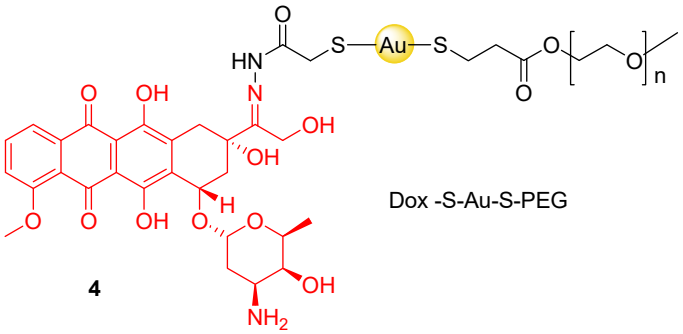

Figure 4. Gold nanoconjugate with Dox and PEG attached using thiol group reported by Aryal et al[30].

Wang et al. reported similar tethering of Dox to Au-NPs. However, they attached Dox on the terminal end of Au-attached PEG polymer through hydrazone linkage (Figure 5).[31] The Dox-Hyd@AuNPs showed better drug accumulation and retention in multidrug-resistant MCF-7/ADR cancer cells in comparison to free Dox. The Dox-Hyd@AuNPs released Dox in response to the pH of acidic organelles following endocytosis, opposite to the non effective drug release from Dox-tethered Au-NPs *via* the carbamate linkage (Dox-Cbm@AuNPs). Dox-Hyd@AuNPs therefore significantly enhanced the cytotoxicity of Dox and induced elevated apoptosis of MCF-7/ADR cancer cells. The Dox-Hyd@AuNPs represents a model with dual roles in overcoming multi drug resistance (MDR) in cancer cells and probing the intracellular release of drug from its delivery system. Involvement of hydrazone bonding in above systems with Au-NPS provided the expected acidity based drug release profile.

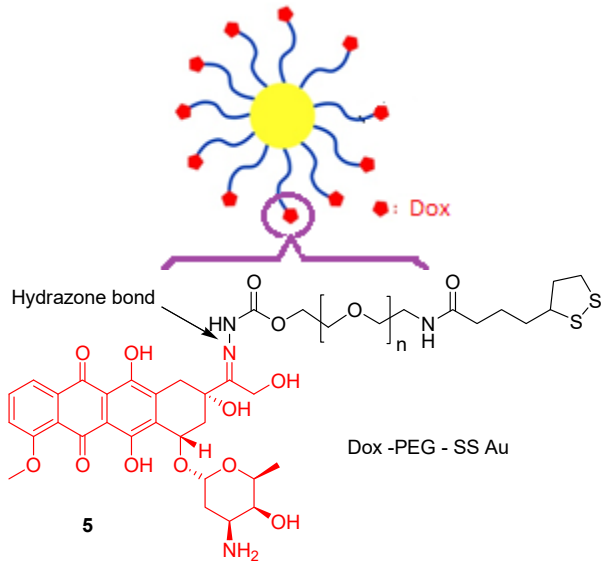

Figure 5. Representation of Dox attachment to Gold nanoparticle using Hydrazone linkage via functionalized PEG linker reported by Wang et. al.[31].

Direct adsorption of Dox on the AuNPs is possible in the acidic medium as reported by Mirza et al.,[32] however, the fate of directly adsorbed Au-Dox is uncertain due to lack of evaluation in *in vivo* or *in vitro* conditions. Swiech et al. also reported similar observation where they prepared Dox-loaded AuNPs using either peptide (amide) linkage or hydrazone linkage. The antiproliferation assay and confocal microscopy studies revealed that the bond between the AuNPs and Dox determined the pathway of cell death. As studied with MTT assay performed on two cell lines (A549 and HeLa), the cell death was apoptotic in the case of Au-Dox having peptide bonding, and it was sudden necrotic cell death when Au-Dox were attached via hydrazone bond.[33]

2.1.3. THROUGH THE AMIDE/CARBAMATE BOND

Du et al. reported the Dox-Au conjugates containing a carbamate linkage. The various carbamate, hydrazine, and formyl ester linked Dox derivatives with PEG or 4-mercaptobenzyl alcohol were chemically synthesized having sulfur at the terminal end, as shown in Figure 6. The terminal sulfur was used for loading the Dox derivatives on the Au nanoparticles in the presence of mPEG thiol.[34]

In vitro antiproliferation assay of synthesized compounds on ovarian cancer (A2780) cell line showed the IC_{50} value (in nM) of **6** (31±5nM), **7** (10±4nM), **8** (28±3nM), **9** (11±5), **10** (11±1nM) and Dox **1** (26 ± 3nM) indicating the lower values for **7**, **9**, **and 10** compared to Dox. Compound **6** was found to be stable at physiological pH 7.4 (37 °C) as well as at acidic condition pH 4.6 (37 °C) indicative of negligible release of Dox under both conditions. Compound **7** showed the faster release of Dox at pH 4.6 (37 °C). However, only 55% of this leads to free Dox. The group prepared the AuNPs with selected compound **6** with an average diameter of 41 nm and loading of 0.78 mg per 1 mg of AuNP. The stability of compound **6** was observed during *in vivo*

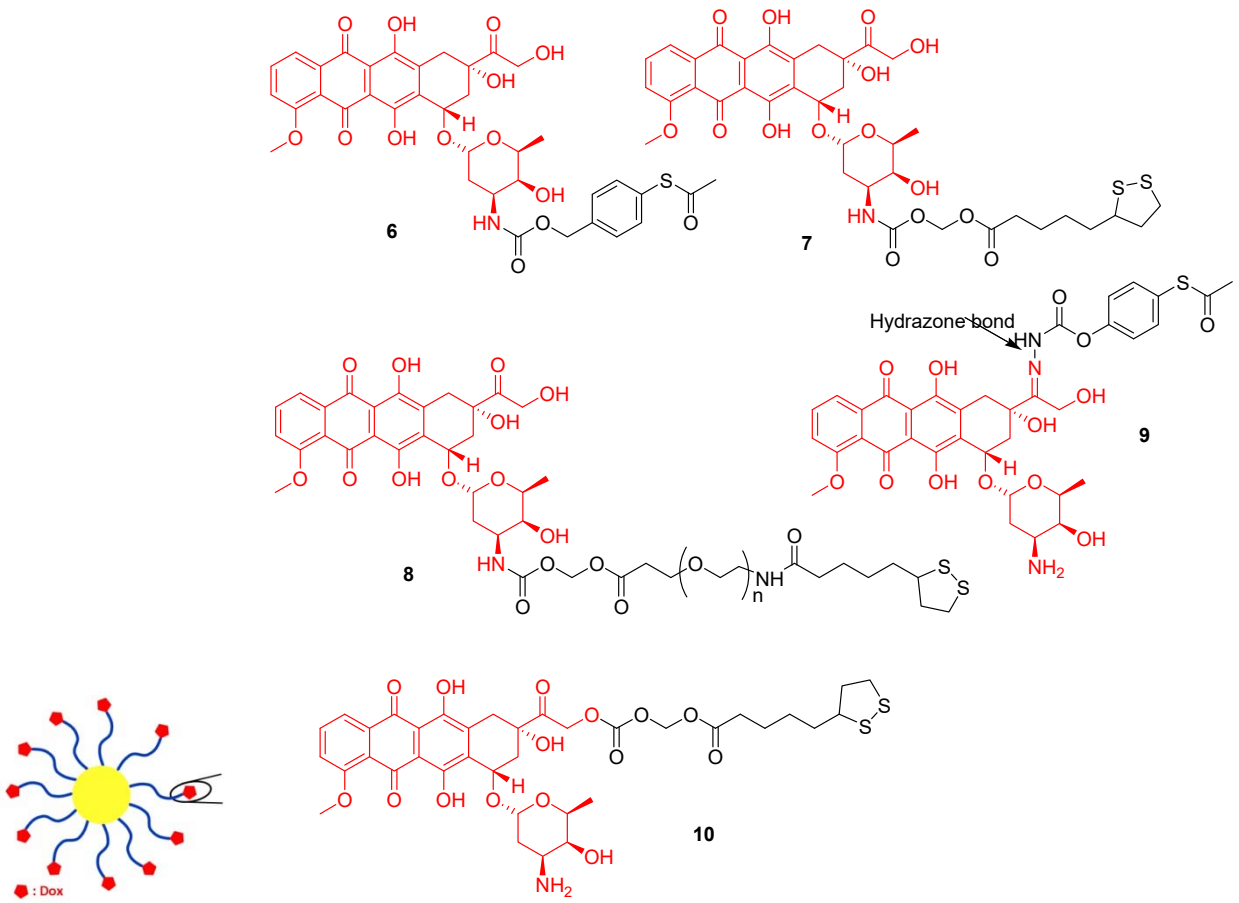

Figure 6. Different Dox-Au derivative attached through carbamate (**6, 7, 8**), Hydrazone (**9**) and 14'-OH formyl ester (**10**) linkage as reported by Du et. al.[34]

experiments where significantly lower plasma levels of Dox were observed in plasma samples from mice given Au-**6**-Dox (Au nanoparticle with compound **6**) compared to plasma samples for mice given free Dox. Due to the lack of further experimentation for the release of Dox from nanoparticles in cancerous cells in this report, the final fate of these derivatives with AuNPs remains vague.

To conclude with different AuNPs reports above, the covalent conjugation of Dox has been done directly on the nanoparticles or polymer coated Au-NPs using disulfide linkage, hydrazone, and carbamate bond formation. The reported studies provide details of conjugation and release studies while fate in *in-vivo* condition is uncertain for the reported Au-NP-conjugate systems.

2.2 Iron Nanoparticles

Nanoparticles of Iron as well as that of oxides of Iron have been studies and applied in various fields. The Iron or Iron oxide NPs retain the magnetic properties of Fe, which provide these nanoparticles a unique property for application in different fields. The usefulness of magnetic tracking of NP conjugates and controlling the distribution of magnetic NPs in reaction systems or biological systems provide robust applicability of these NPs in different systems.[35] The enhanced magnetic properties of these NPs has made them to be referred as Superhigh magnetization nanocarriers (SHMNCs). The magnetic property make them suitable for tracking using the magnetic resonance imaging (MRI) or magnetic resonance spectroscopy (MRS). Compared to gold, the economic cost of Iron nanoparticles make these easily available, giving impetus for enhanced exploration of these NPs.

The Iron or Iron oxide NPs has been studied for delivery of Dox drug using the constructs with these nanoparticles having the coating of organic molecules or polymers which is used for covalent linkage of Dox. The surface coating help in controlling other pharmacological properties as well and so their selection optimization depend according to end application. The linking of Dox on the surface coated nanoparticles achieved using amide, hydrazone and other linkage.

2.2.1 Using Amide bond

The conjugation of Dox to iron nanoparticles has been done in a similar way by coating the nanoparticles with polymer layers. Hua et al. coated the poly[aniline-co-sodium-N-(1-one-butyric acid)aniline] on superparamagnetic iron oxide (Fe_3O_4) nanoparticles (SPION) or also referred to as Superhigh magnetization nanocarriers (SHMNCs).[36] The activated carboxyl group was generated at the surface of the polymer. The activated carboxyl group coupled to the primary amine group of Dox to form SPION-Dox particles via amide bond **11** (Figure 7).

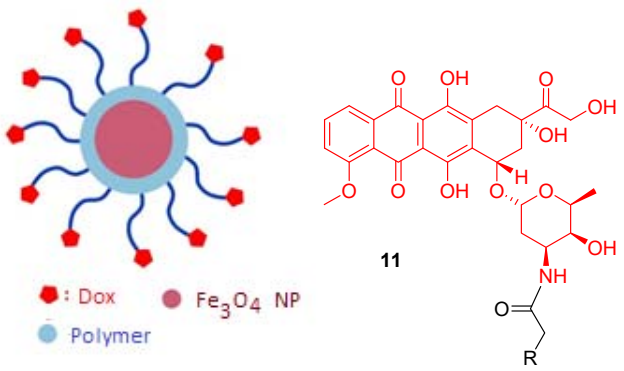

Figure 7. Structure of Fe-SPION-Dox conjugate reported by Hua et al.[36] SHMNCs: SuperHigh-Magnetization Nanocarriers.

According to their report, the quantity of Dox loading was 271 µg/mg of Fe-SPION-Dox system corresponding to 27.1%w/w loading. The higher loading compared to other delivery systems is believed to be due to the higher surface area of SPION. The release kinetics of the Dox from Fe-SPION-Dox conjugate was not included in the report. The high R2 relaxivity (434.7 $mM^{-1}S^{-1}$) of Fe-SPION-Dox conjugate is useful in tracing it quantitatively in animal body/organs by MRI. The cytotoxicity of Fe-SPION-Dox in bladder cancer MGH-U1 cells was believed to be due to direct intercalation or free radical generation by conjugated Dox in Fe-SPION-Dox. The cytotoxicity was observed to enhance when magnetic therapy was applied. The observed cytotoxicity of Fe-SPION-Dox described in the report either *in vitro* or *in vivo* is mainly with intact Fe-SPION-Dox alone or complemented by magnetic therapy as it is silent about the release of Dox from the conjugate.

In a similar way, Fang et al. also introduced amide bond linkage in (poly(beta-amino ester) PBAE **13** polymer for direct incorporation of Dox via its primary amine group. PBAE **13** is PEG-based copolymer[37] with (di(ethylene glycol) diacrylate) DEGDA **12** and dopamine) coated around Fe nanoparticles (Figure 8).[38]

The polymer designed by Fang et al. for loading of Dox on SPION nanoparticles contained ester bonds in it for releasing the Dox at lower pH. Dox was introduced as an integral part of PBAE polymer through the primary amine group of Dox. The final structure contained the tertiary amine (from Dox, PEG or DPA) and ester bonds. Fang et al. stated that Dox, as incorporated via stable amine linkage, would help in preventing the premature release of Dox from the system and allows nanoparticle conjugate to reach and accumulate in the tumor site. Dox-containing polymer was loaded on SPION nanoparticles through conjugation. The high Dox contents in the polymer (9.5% w/w of the total polymer) lead to the generation of nanoparticles with 679 µg of Dox per 1 mg of iron. As SPION-PBAE system contained pH sensitive ester back bone, the acidic pH promoted the degradation of the polymer and released of Dox component. At pH 7.4, over 30% of Dox component got released from polymer after 72 h while 40% was released at pH 6.4 and 55% at pH 5.5.

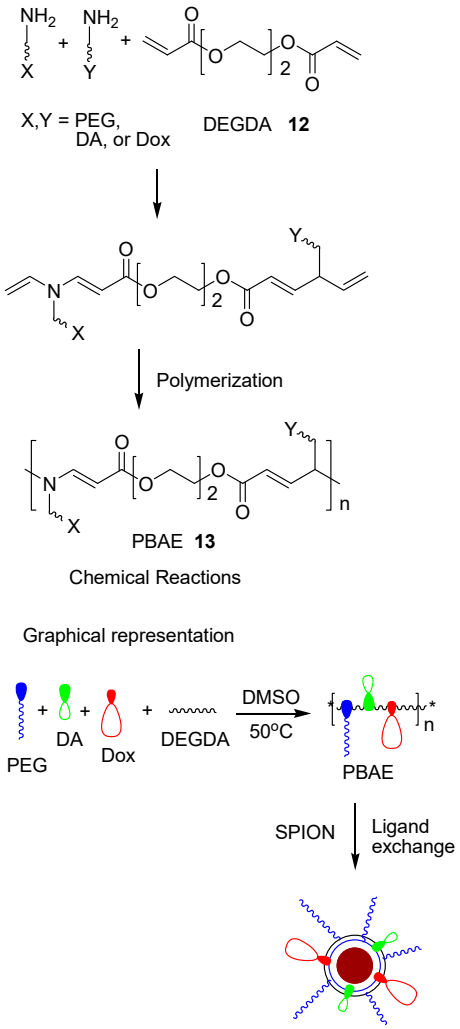

Figure 8. Illustration of PBAE synthesis and introduction on SPION nanoparticle surface. PEG-NH_2 (PEG), Dopamine (DA), Doxorubicin (Dox) and (di(ethylene glycol) diacrylate) DEGDA**12** is reacted at 50°C in DMSO to obtain the Dox-loaded PBAE **13** polymer which is further transferred to SPION nanoparticles through ligand exchange as reported by Fang et.al.[38]

2.2.2 Using Hydrazone Bonds

Kievit et al. used polyethylene amine (PEI) for the incorporation of Dox and then docking this conjugate on the PEGylated SPION.[39] Dox was loaded in high quantity (i.e., 1089 molecules per nanoparticle) using hydrazone bonding between Dox and PEI (Figure 9). Hydrazone bond being pH sensitive would be beneficial in releasing the Dox at the tumor site. However, Dox was loaded using PEI instead of the direct polymer layer of SPION. Thus, the PEI molecules get released and would cause the cytotoxicity as any released PEI penetrates in the nucleus and prevents the normal transcription process. The release kinetics of Dox showed a burst effect in the first 1h followed by a plateau at all pH ranges of 4.5 to 7.5, probably because of the release of PEI from the PEG – SPION. The hydrazone bonding facilitated the release of Dox at lower pH while at other pH values it did not affect the release kinetics (the unusual burst release from

nanoparticle). However, the total Dox released did not exceed the 30% of loading probably due to hydrophobic interactions between Dox and polymer after cleavage of hydrazone linkage. PEI itself acts as buffering material, and in this capacity, it prevents the normal acidification of endosomal vesicles and degradation of endosomal contents.

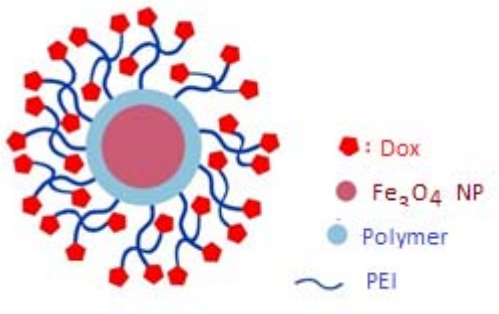

Figure 9. Depiction of the conjugation of Dox with PEI and loading on the PEGylated SPION reported by Kievit et al.[39].

2.3 Silver Nanoparticles

Silver nanoparticles [Ag NPs] are known to induce apoptosis or necrosis in numerous cell types.[40] Hekmat et al. studied the combined effects of silver nanoparticles (Ag NPs) and Dox on structural changes in DNA and their corresponding inhibitory roles in the growth of T47D and MCF7 cells.[41] The values of observed binding constants for DNA-Dox, DNA-Ag NPs, and DNA-Dox-Ag NPs complexes revealed that the combined Dox and Ag NPs interact more strongly as compared to either Dox or Ag NPs alone. The combination of Dox+Ag NPs significantly disturbed the molecular structure of DNA and induced the formation of DNA condensed form (ψ type). The Ag NPs also enhanced the cytotoxic effect of Dox on MCF7 cells and T47D cells, having a significant difference with Dox or Ag NPs alone.[41]

Benyettou et al. used Ag NPs for dual delivery of Dox and alendronate (Ald) **14**to cancer cells towards synergistic effect by simultaneous improved delivery of both drugs (Figure 10).[42] The Ag NPs synthesized by bisphosphonate mediated synthesis were coated with bisphosphonate Ald, which was further used for conjugation of Dox through imine bond. Rhodamine B conjugated

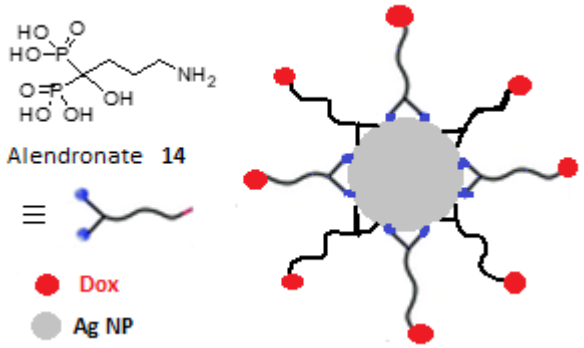

Figure 10. Dox loading on Ag NPs using Alendronate (hydrazone bonding).

to Ag-Ald nanoparticle (in place of Dox) was used to find out the mechanism of uptake of nanoparticles by confocal fluorescence microscopy, which showed that cellular uptake of nanoparticles is through macropinocytosis and clathrin-mediated endocytosis. Higher uptake and acid-mediated release of Dox (by hydrolysis of imine linkage) resulted in the greater antiproliferative activity of cancer cells *in vitro* compared to the individual activity of Ald or Dox.

Ag NPs have also been used in chemo-photodynamic therapy nanoconjugates. The nanoconjugate of silver/graphene quantum dots (CdS) and Dox showed improved cytotoxicity against cancer cells with better cardioprotective effect.[43] Moreover, it was reported that grapheneoxide@Ag-Dox-DSPE-PEG2000-NGR (GO@Ag-DOX-NGR) nanoconjugates showed excellent chemophotothermal therapeutic efficacy, tumor-targeting properties, NIR laser-controlled drug-releasing functions, and X-ray imaging ability in an *in vivo* murine tumor model.[44]

2.4 Quantum Dots

Quantum dot nanocrystals are different photoluminescent nanodimensional materials typically synthesized from binary combinations of a variety of semiconductor materials (ZnS, ZnO, CdS, CdSe, InP, CdTe, PbS, PbTe). For drug delivery and other biological applications, the quantum dots are generally first loaded with biomolecules (peptides, PEG, small molecules, aptamers (RNA, DNA fragments), etc.) through metal-affinity interactions or disulfide bond, which help in biorecognition, biophysical properties[45] controlling, and target delivery.[46] The first loading may generate surface ligands, such as carboxylic acid or amine group, which can further be used for other biomolecules/drug attachment.[47] The Quantum dots have dual benefits of serving as delivery vehicles (due to nanomolecular size) and *in vitro* cellular imaging of nanoconjugate (due to photoluminescence). This multifunctional design system of Quantum Dots for simultaneous imaging and delivery of therapeutic agents is an advantageous system as this dual task system represents a substantial challenge for other types of nanocarriers.[48]

2.4.1 QD-Dox Conjugates

The QDs have size-tunable photoluminescence spectra with high molar extinction coefficients (~10 – 100 times that of organic dyes). This provides optimal tissue imaging for fluorescent excitation while there may be low background noise from water, proteins, and other endogenous fluorophores. These properties also allow the QDs to function as excellent fluorescence resonance energy transfer (FRET) donors. QDs have been shown to be excellent donors for both organic dye and fluorescent protein acceptors. On conjugation of Dox with QD, QD-Dox FRET takes place. As Dox is fluorescent, it partially quenches the QD photoluminescence via FRET and once inside the cells, the free Dox fluorescence is also self-quenched on DNA binding. Intracellular release of Dox from QD would be signaled by a concomitant increase in fluorescence of both the QD and Dox; correlating with the reduction of FRET. The targeted cell line would thus fluorescently be labeled in two colors (QD and Dox) as a result of this delivery strategy and thus help in

monitoring the cellular activity of QD-Dox conjugate. In one example, Bagalkot et al. assembled a CdSe/ZnS QD-aptamer conjugate capable of targeting prostate cancer cells for drug delivery.[49]The QD-aptamer-Dox conjugate showed partial quenching of the QD PL via FRET. The Intracellular delivery of Dox cargo was signaled by a concomitant increase in both the QD and Dox fluorescence correlating with the reduction of FRET. The targeted cell line was thus fluorescently labeled in two colors (QD and Dox). In this configuration, the QD provides multiple roles, including nanoscaffold for aptamer and drug attachment, fluorescent marker in the conjugate, and part of the FRET signal in drug release.[48]

2.4.1.1. HYDRAZONE LINKAGE

R. Salva et al. reporteddrug delivery system that consists of (1) QD as a carrier, (2) Dox as an anticancer drug conjugated to QD via a pH-sensitive hydrazone bond, and (3) aptamer targeted to mutated MUC1 mucin as a targeting moiety/penetration enhancer for imaging and treatment of drug-resistant ovarian malignances. The quantum dot-mucin1 aptamer-Dox (QD-MUC1-Dox) conjugate was synthesized by conjugating the QD with a DNA aptamer specific for mutated MUC1 mucin overexpressed in many cancer cells including ovarian carcinoma followed by attaching of Dox to QD via a pH-sensitive hydrazone bond selected for drug release in the acidic environment inside cancer cells. The 5′-amine terminated MUC1 DNA aptamer [5′-GCA-GTT-GATCCT-TTG-GAT-ACC-CTG-G-3′] was attached to carboxyl terminated quantum dots (QD-COOH) Cd/ZnS QD first, followed by hydrazine treatment to generate amine on QD, and then Dox was attached via hydrazone bond (Figure 11). As expected, the conjugate through hydrazone bond remained stable at neutral and slightly basic pH and underwent rapid hydrolysis in mildly acidic pH. Confocal microscopy and *in vivo* imaging studies showed that the developed QDMUC1-DOX conjugate had higher cytotoxicity than free Dox in multidrug-resistant cancer cells and preferentially accumulated in ovarian tumor.[50]

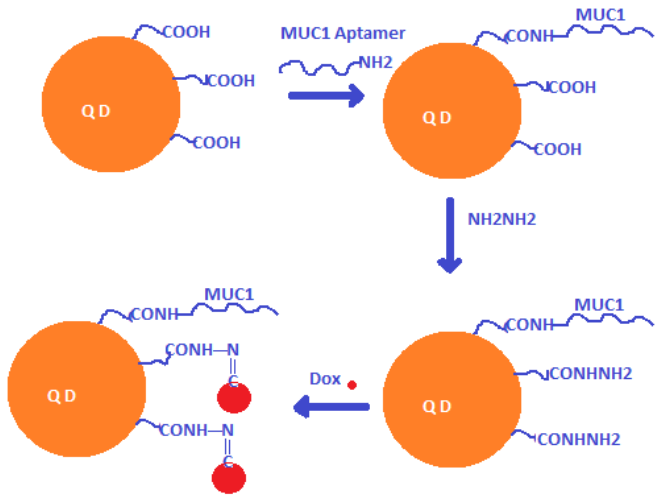

Figure 11. Loading of QD with Aptamer and Dox using hydrazone bond(QD-MUC1-Dox) as reported by Salva et.al.[50].

The QD-MUC1-Dox showed better uptake in ovariantumorcompared to unmodified QC in i*nvivo* imaging in the mice. This study provided a base for using aptamer for targeted delivery of conjugates in place of peptide/antibody-based conjugates. The conjugate loading with Dox via hydrazone bond indicated a better release of drug in the tumor site (Figure 12).

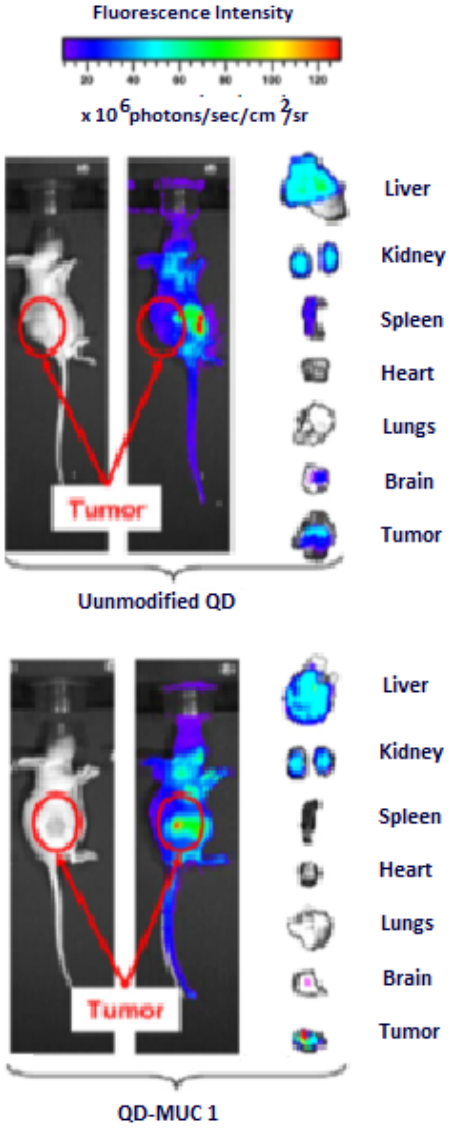

Figure 12. Biodistribution of non-modified quantum dots (QD) and tumor-targeted by MUC1 aptamer QD (QD-MUC1) conjugate. Image reproduced from the report by Salva et. al.[50] with permission (Copyright Elsevier).

The ZnO quantum dots surface can be functionalized with different biomolecules, and because of its high photoluminescence find application in bioimaging.[51] In addition to bioimaging, ZnO QDs have also been evaluated as a platform for targeted and pH-responsive intracellular delivery of Dox. The cancer targeting feature of carrier conjugate has been endowed by conjugating folic acid[52] on to the surface of ZnO–NH_2 QDs *via* an amidation reaction. Dox is then loaded onto the folic acid functionalized ZnO QDs through metal complexation reaction of Dox with ZnO.

Drug-loaded ZnO-FA QDs remain stable at physiological pH but could disintegrate in the mildly acidic intracellular environment of cancer cells. Compared to the conventional drug nanovector, ZnO-FA QDs themselves provide a significant therapeutic activity supplemented by the additional release of Dox from the conjugate. Combined Dox and ZnO QDs have been proposed to be more efficacious than either alone. Further, photoluminescence of ZnO nanoparticle can be used for tracing the nanocarrier, thus providing simultaneous targeting (with folic acid), diagnosis (with ZnO), and therapy (with FA and Dox) of cancer cells.[53,54]

In generalization, Quantum Dots possess unique structural and surface properties, such as tunable and uniform size, flexible drug linking, and doping mechanisms, large surface to volume ratio and a wide spectrum of surface reactive groups, which make these nanoparticles a suitable vehicle for targeted and traceable drug delivery systems.[55] The QDs have the unique combined property of being used as a delivery vehicle as well as a tool for drug screening in a single system.[56] However, as the majority of QDs are made with heavy metals and thus, may generate long-term toxicity. The toxicity concerns can be mitigated through high-quality QDs prepared from relatively non-toxic compounds (e.g., silicon and carbon).[57] For mitigation of toxicity and to utilize properties of targeting systems, such as folic acid or combination with other nanosystems, such as carbon nanotubes,[58] chitosan,[59] graphene,[60] etc. has also been reported. The systematic study is still warranted for maintaining a useful concentration of the drug in the targeted tissue while preventing toxicity due to QD.

3. SILICA NANOPARTICLES

The silica nanoparticles have wide significance due to their excellent *in vivo* stability profiles, which makes these inorganic nanoparticles fit for medical and biological applications. Compared with other nanoparticles (organic)drug carriers, mesoporous silica nanoparticles (MSNs) possess some unique properties such as high specific surface area, large pore volume, tunable pore structure, and stable physicochemical properties.[61] MSNs have been intensively investigated in various fields including controlled drug delivery, biosignal probing, gene delivery, biomarking, and other biomedical applications.

Dox delivery has been mostly investigated by non-covalent adsorption on the (mesoporous) silica nanoparticles. The report by Shen et al[61] showed higher loading of Dox on smaller size MSNs, such as Dox loading capacity of MSNs with 120nm size could reach 306 mg Dox per gram MSNs 120, indicative of high specific surface areas. Although, higher loading could be achieved with porous silica nanoparticles, the release of Dox from loaded nanoparticles was very less, i.e. ~ 20% in 24 h and reaching a maximum of ~25 release in 48h. Also, the rate of release was fast enough, i.e. it was released exponentially in the first 12 h and after that negligible slow release. These release kinetics makes MSNs unfit for clinical applications. Similar work to evaluate the pore size of mesoporous silica nanoparticle from the same research group authored by Guo et al[62] reported similar behavior of Dox release from silica nanoparticles.

Further, surface modifications supported secondary coverings have also been introduced for improving the surface kinetic properties of silica nanoparticles. Meng et al.[63] have reported the functionalization of the silica particle surface with a phosphonate group to allow electrostatic binding of Dox to the porous interior and releasing Doxdrug by acidification of the medium under abiotic and biotic conditions. The group has also used phosphonate modification for exterior coating with the cationic polymer, polyethyleneimine (PEI) for evaluation in contemporaneously delivery of Pgp siRNA. Compared to no surface modification, COOH-functionalized, NH_2 modification; the surface phosphonate functionalized silica nanoparticles showed higher Dox loading. Dox release from Phos-MSNs showed pH-dependent release kinetics with nearly 40 % release in 360 min and approximately 50% release in 720 min under acidic conditions while it was negligible under neutral phosphate buffer conditions (Figure 13).

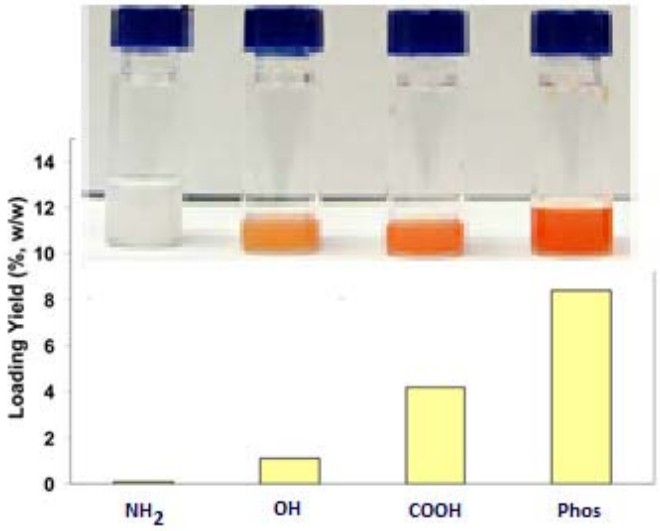

Figure 13. Higher loading of Dox on Phos-MSNs compared to other modifications. Adapted from a report by Meng et al[63] with permission. (Copyright ACS)

The surface modification with PNiPAM/AA (poly(N-isopropylacrylamide) (PNiPAM)-co-acrylic acid (AA) hydrogel) has been reported by Hu et al[64] for thermal as well as pH-controlled loading and release of Dox from modified silica nanoparticles. Dox release showed comparatively more release at pH 5 compared to pH 7; however, nearly 60-65% of loaded Dox released within 5 h under all conditions, after which showed only 5-10% release upto 25 h. This limits the application of this system requiring the sustained release of Dox, the key requirement of the drug delivery system. Various other molecules, such as PEG[65] and aminopropyl,[66] have also been examined with similar inferences.

The silica nanoparticles have alsobeen loaded with dual compounds including Dox and one another organic molecule (such as for phthalocyanine) for photodynamic therapy along with the pH-controlled release of Dox from the silica conjugate nanoparticles.[67]

4. CARBON NANOSYSTEMS

Nanometer-sized carbon allotropes viz. carbon nanotubes, fullerene, and graphene with the capability to cross the cell

membrane and non-toxic behavior have led to their evaluation in various biological applications, including drug delivery. Carbon nanosystems differ in their structural morphology and physical surface properties, which help in developing their potential analysis in applicability in a suitable field. Application of these carbon nanosystems in drug delivery, particularly the delivery of various anti-cancer drugs, using covalent and non-covalent drug conjugation on the surface, has generated a wide literature covering different aspects. The conjugate systems for delivery of Dox have been summarized below.

4.1. Carbon Nanotubes

The carbon nanotubes (CNT) with 1-5 nanometer diameter and spanning the length 20-200nm (including single walled, multiwalled and short carbon nanotubes) are folded jointed sheets of graphene layer with the high surface area and unique physical properties like high mechanical strength and electrical conductivity.[68] Due to the ability to cross cell membrane permeability of CNTs, these have been used for delivery of various drug molecules.[69,70] In case of Dox, most of the reports used non-covalent loading of Dox on CNTs due to strong adsorption by π-π stacking. The release kinetic and incomplete release of Dox from CNT-Dox conjugate remains questionable for the end application. The CNT surface functionalization (like with –COOH group) and also the CNT surface wrapping with other polymers have been reported for pH-controlled release and simultaneous photothermal therapy with similar end inferences.[7172]

The covalent functionalization of CNT (multiwalled CNT) with polystyrene for loading with Dox has been achieved through hydrazonebonding by Le et.al.[73] for pH-controlled release of Dox from conjugate (Figure 14).

In this report, the loading through covalent functionalization was more (~18%) compared to pristine MWCNT (negligible). The release kinetics showed that only ~20% Dox was released from the MWNT/PSMA-DOX at pH 7.4 after 24 h. The release of DOX was significantly increased at pH 5.0 with 56% of DOX released after 24 h. The results indicated that acid-sensitive hydrazone bond was relatively stable at pH 7.4 but cleaved at pH 5.0, and thus Dox could diffuse out from MWNTs more in acidic medium. The majority of release (in both cases neutral as well as acidic pH) occurred within 12hours, limiting the efficacy of application of this system.

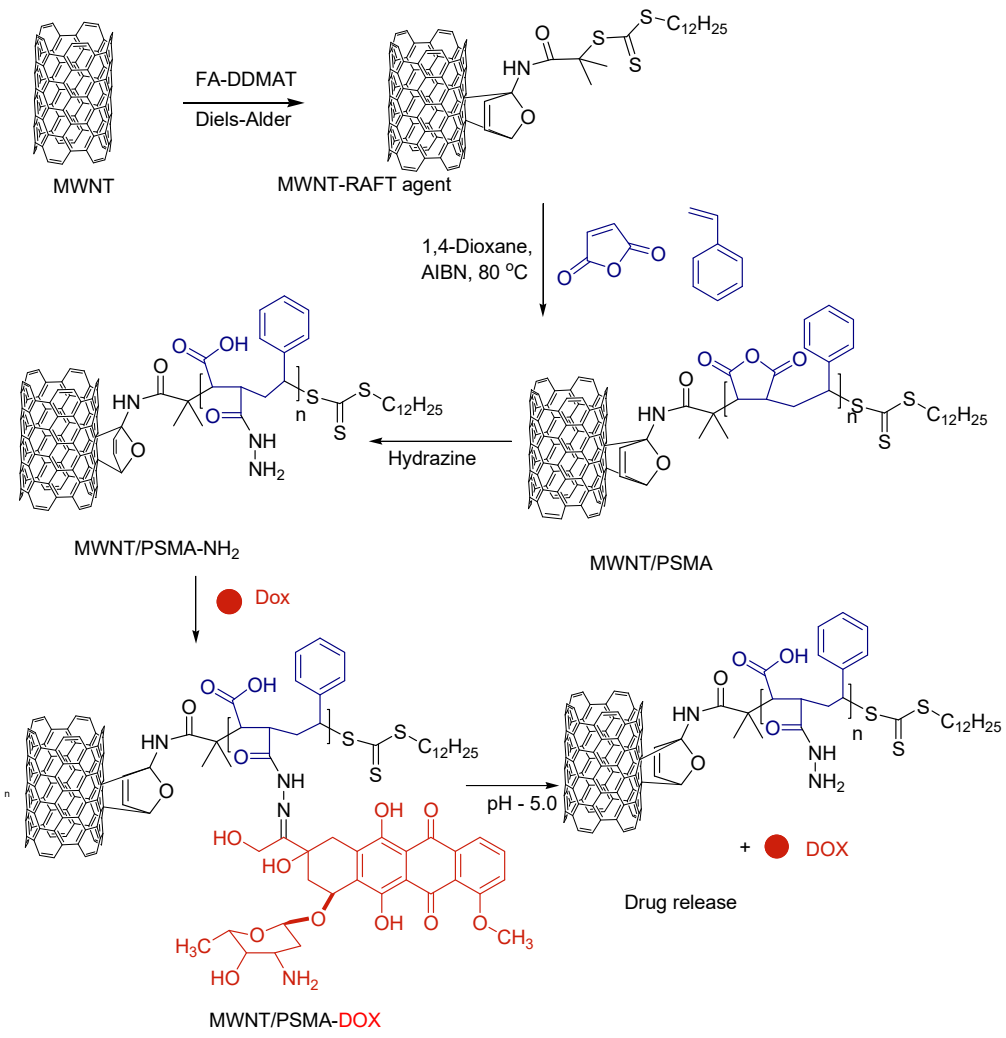

Figure 14. Indicative representation of covalent loading of Dox on MW-CNT as reported by Le et. al.[73].

4.2. Fullerenes

Fullerenes are spherical carbon structures in nanometer dimensions and have good cellular uptake profile due to nano size. The fullerenes have been chemically functionalized for loading of Dox and evaluated for therapeutic application via the amide linkage by Chaudhary et al.[74] (Figure 15). The report indicated the minor difference in cytotoxicity of Dox and Fullerene-Dox conjugate. The release and lower cytotoxicity results can be compared with the unhydrolyzable amide linkage of Dox-Fullerene conjugate. Further, the *in vitro* activity obtained and reported was at much higher concentration of 5 μM, which indicated the reported cytotoxicity in different cells in *in vitro* conditions might be due to less release with high concentration effect over the IC_{50} for free Dox molecules.

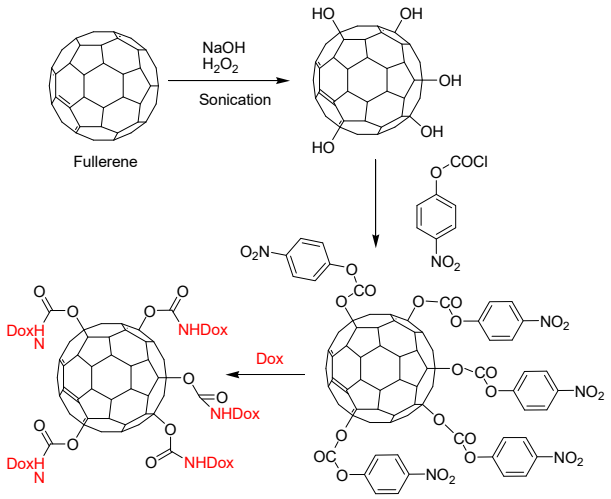

Figure 15. The loading of Dox on fullerene via amide linkage as reported by Chaudhary et.al.[74]

Zhao et al. have used RGD peptide for improving the uptake of the Fullerene-Dox conjugate in lung cancer cells.[75] The *in vitro* results demonstrated that Dox-C82-cRGD nanoparticles showed preferential cellular uptake in non-small lung cancer cells as compared with Dox-C82 and in much higher uptake in comparison with only Dox incubated cells. The higher uptake of Dox-C82-cRGD had significant improvement in cytotoxicity to cells at a low dose.

4.3 Graphene

The graphene, though parent to all carbon nanomaterials, is most recent among discovered carbon nanomaterial and is getting increasing research attention to explore this new material for drug delivery along with numerous other applications. Graphene is a single layer of sp^2 hybridized carbon atoms arranged in a planer honeycomb like two-dimensional (2D) crystal lattice.[76] It has evoked enormous interest throughout the scientific community since its first appearance in 2004[77] as due to its unique structure and geometry, graphene possesses remarkable physical–chemical properties including half-integer quantum Hall effect, ballistic electron transport, a high Young's modulus, excellent electrical and thermal conductivity, high fracture strength, fast mobility of charge carriers, large surface area, and good biological compatibility.[78] These properties make graphene ideal materials for evaluation and application in a broad range of applications, ranging from quantum physics, nano-electronics, nanoenergy materials research, chemical application in nanocatalysis as well as engineering field applications of nanocomposites materials and biological materials.[79]

In the field of nanobiotechnology and nanomedicine,[80,81] graphene, graphene oxide and their composites with other materials have emerged as new biomaterials for explorations in different exciting research advances in area of biological sciences, biotechnology and medical sciences such as development of a new generation of biosensors, nanocarriers for drug and gene delivery; and development of nanoprobes for cellular organelles, cells and biological imaging.[60,82]

The graphene has been evaluated for the delivery of Dox by direct adsorption on the graphene surface as well as by intermediate molecules-based attachment. The non-covalent adsorption brought the good loading due to stacking impact of Dox and Graphene while the release profile of Dox from complex has not been suitable for the application. The molecular attachment intermediated by molecules, such as polymers, PEG and other has also been attempted for delivery studies of Dox giving the mixed results mainly depending upon the characteristics of interaction between Dox and intermediating molecules.[83,84]

5. Dendrimers

Dendrimers are used as a delivery vehicle for various anticancer drugs. The structure and tunable surface functionality of dendrimers allow the encapsulation/conjugation of multiple entities, either in the core or on the surface, rendering them ideal carriers for various anticancer drugs.[85]

Jesus and colleagues[86] explored the possibility of a 2,2-bis (hydroxymethyl) propanoic acid-based dendritic scaffold as a delivery carrier for Dox *in vitro* and *in vivo*. This dendritic nanoformulation, which contains Dox covalently bound through a hydrazone linkage to a high molecular weight 3-arm polyethylene oxide; exhibits reduced cytotoxicity *in vitro*. However, *in vivo* biodistribution experiments showed minimal accumulation of Dox-dendrimer conjugate in vital organs, including the liver and heart, and increased the half-life of Dox compared to the free drug. Thus, it was hypothesized that proper choices of nanocarrier systems could increase the circulation half-life to effectively exploit the enhanced permeation retention (EPR) effect phenomenon and thus have potential to increase the efficacy of the drug.

In an attempt to improve the efficacy of Dox, Lai and colleagues[87] utilized photochemical internalization (PCI) technology for site-specific delivery of membrane-impermeable macromolecules from endocytic vesicles into the cytosol. PCI technology has been demonstrated to successfully enhance the cytotoxicity of cancerous tissue by destroying the cytoplasmic membrane and facilitating the release of macromolecules entrapped in cytoplasmic vesicles. PAMAM dendrimers were conjugated to Dox through the amide (PAMAM–amide–Dox) or the hydrazone (PAMAM–hyd–Dox) bonds. Two different PCI strategies referred to as 'light after', and 'light before', where exposure to light is either after or before treatment with Dox, respectively, were applied to evaluate the cytotoxic effects of these Dox PAMAM conjugates against Ca9-22, gingival carcinoma, cells. It was observed that only the 'light after' PCI treatment significantly increased the nuclear accumulation of Dox from the PAMAM-hyd-DOX conjugates and thus exhibited higher cytotoxicity, probably due to the synergistic effects. Both PCI strategies failed to improve the cytotoxicity of PAMAM-amide-DOX conjugates.

6. Lipophilic Systems (Fatty Acid Conjugates)

Dox is a highly hydrophilic organic drug, and this property could be leading to its pharmacological profile, biodistribution,

and excretion kinetics. Small organic molecules could be developed on Dox molecular structure for improving towards desired pharmacological profile. Our laboratory has been actively engaged in pharmacological profile modifications of anti-cancer and anti-HIV drugs using various molecules and concepts of concerted delivery systems.[88–95]

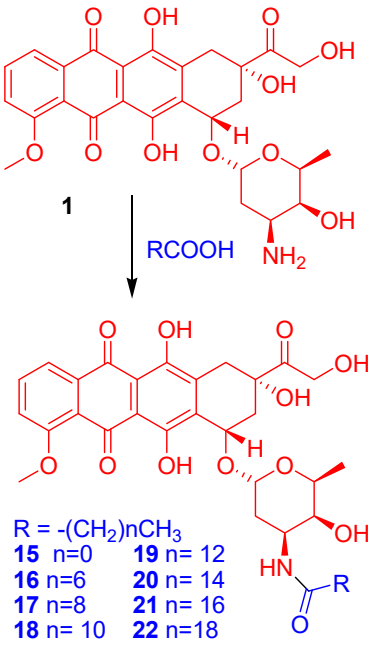

Figure 16. Different amine functionalized lipophilic derivatives of Dox.

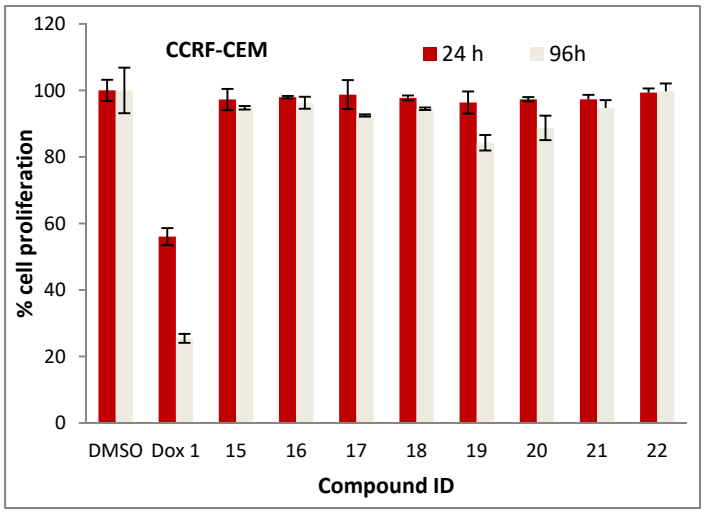

Figure 17. Cytotoxicity profile of Dox and derivatives in cancer cells. Anti-proliferation activity was lost with amidation, as shown in CCRF-CEM Leukemia cells. A similar pattern was observed with MDA-MB-468, SK-OV-3, and HT-29 cells. Figure adapted from ref [96] with permission. (Copyright Elsevier)

Dox has a primary amine on sugar section, which can be functionalized with different very small to large alkyl groups to modulate the lipophilic/hydrophilic characteristic towards improved prolonged availability of the drug for action. Using acylation, different alkyl chain lengths were introduced at the amine group by single step amidation reaction (Figure 16). However, *in vitro* cellular assays showed that these amide derivatives have negligible cytotoxicity compared to Dox (Figure 17). Simply acetylation (-$COCH_3$) of amine (Compound **10**, Figure 16) itself caused the loss of anti-cancer activity as shown by anti-proliferation assay for CCRF-CEM leukemia cells (bar graph for compound 10 in Figure 17). A similar pattern was observed with all fatty amide derivatives of Dox in different cancer cells (MDA-MB-468, SK-OV-3, and HT-29). This loss of activity on amine functionalization indicate the importance of amine group in target binding (Topo-II) and further attributed to the difficulty of amide bond hydrolysis under physiological conditions.[96]

Considering the importance to keep the amine free, the lipophilic derivatives of Dox succinate were synthesized and assessed for anticancer activity and nuclear localization.[97] The free amine at the 3' carbon atom of Dox was first protected with a fluorenylmethyloxycarbonyl (Fmoc) group to prevent conjugation in this position. Fmoc-Dox was then chemically modified at the 14' carbon atom by the addition of succinic anhydride to form the succinate (Figure 18). Fmoc-Dox succinate then underwent esterification or amidation, followed by Fmoc deprotection to generate the respective alkyl ester **27** or amides **23-26** in the form of lipophilic fatty acyl-Dox conjugates (Figure 18). Acyl substituents of various lengths were incorporated into Fmoc-Dox succinate to assess their influences on nuclear delivery and therapeutic activity in human ovarian adenocarcinoma (SK-OV-3), leukemia (CCRF-CEM), breast adenocarcinoma (MDA-MB-468, MDA-MB-361), and colon adenocarcinoma (HT-29) cells.[97]

In vitro antiproliferative experiments showed that the myristoyl amide-Dox **25** and other acyl derivatives possessed a nearly equivalent pattern of antiproliferative activity (Figure 19) to that of free Dox. Notably, the introduction of succinyl group on the 14'C-OH position of Dox (Compound **28**, Figure 18 and Figure 19) did not influence the alternation of antiproliferative activity of Dox in all the cell types used in the assay. For each cell line, **25** was observed to have relatively better cell anti-proliferative activity among the reported fatty acyl-Dox conjugates and has comparable activity when compared to non-conjugated Dox (**1**). Compound **25** has also been assessed for nuclear localization in SK-OV-3 cells. Since Dox fluorescences in the visible electromagnetic region, the subcellular localization of **25**in SK-OV-3 was monitored by fluorescence-activated cell sorter (FACS) analysis. It was observed in FACS analysis that the myristoyl amide-Dox **25** uptake in SK-OV-3 cells showed enhanced cellular uptake by approximately a factor of 3 times in comparison to the uptake of unconjugated Dox. Further, fatty acyl Dox compound **25** gets localized in the cell membrane, the labile succinate ester or amide bonds at the 14' carbon atom are hydrolyzed to release Dox into the nucleus for DNA intercalation. The intercalated Dox–DNA becomes immune to the action of topoisomerase II, which is thus unable to cleave the DNA for replication leading to inhibition of cell proliferation. The improved uptake and thus enhanced antiproliferative activity in various human cancer cells

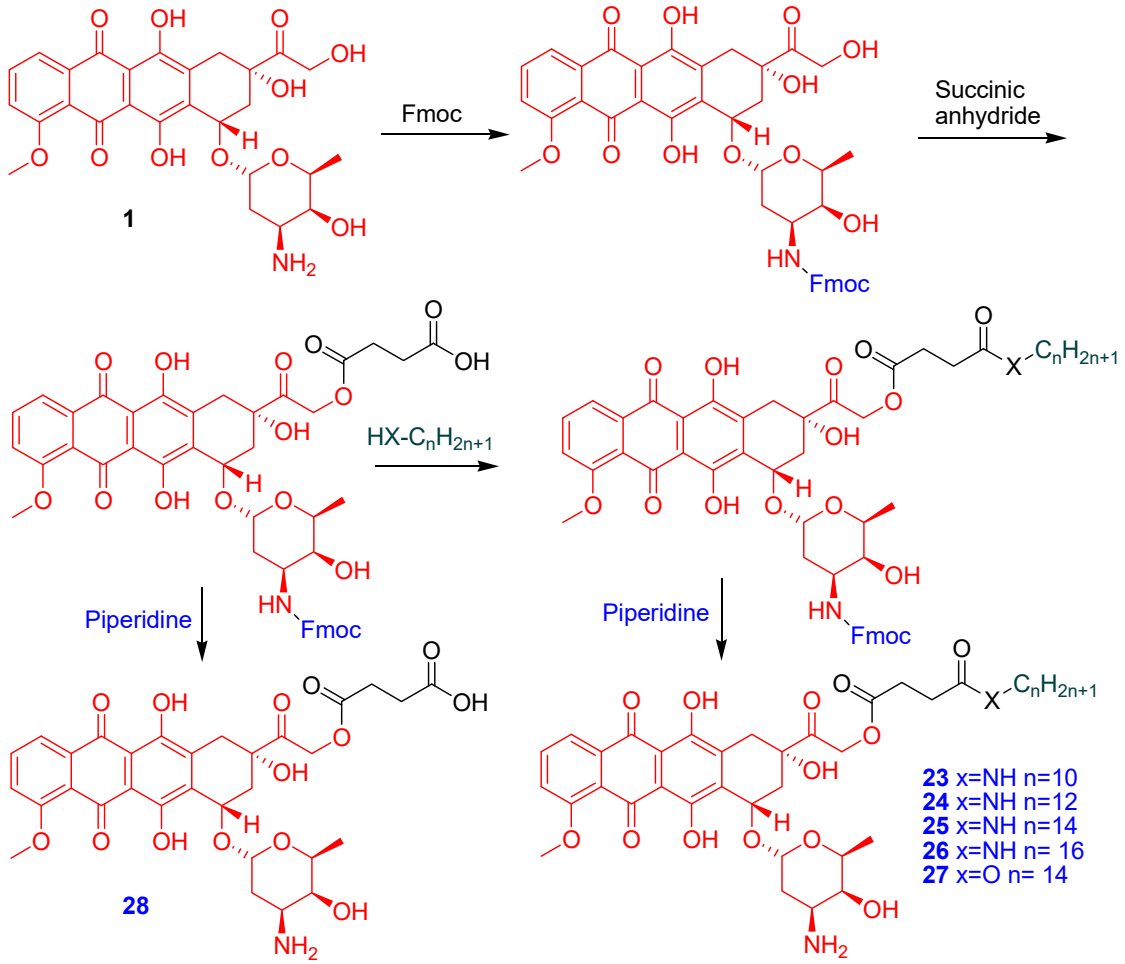

Figure 18. Chemical synthesis of 14-Dox acyl derivatives.

could be due to increased lipophilicity of fatty acyl-Dox conjugates responsible for efficient nuclear localization. Among the reported fatty acyl derivatives, compound **25** possesses the optimal lipophilic chain length for enhanced permeability through the plasma membrane and the optimal balance of hydrophilicity (Dox) and lipophilicity (fatty chain) of the conjugate.

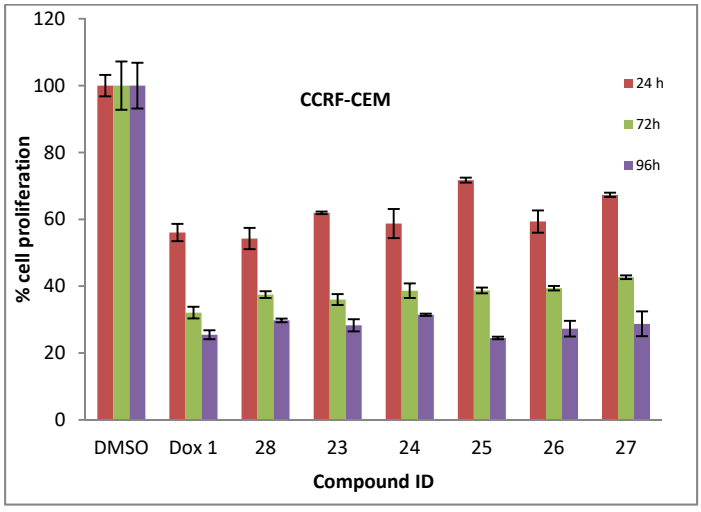

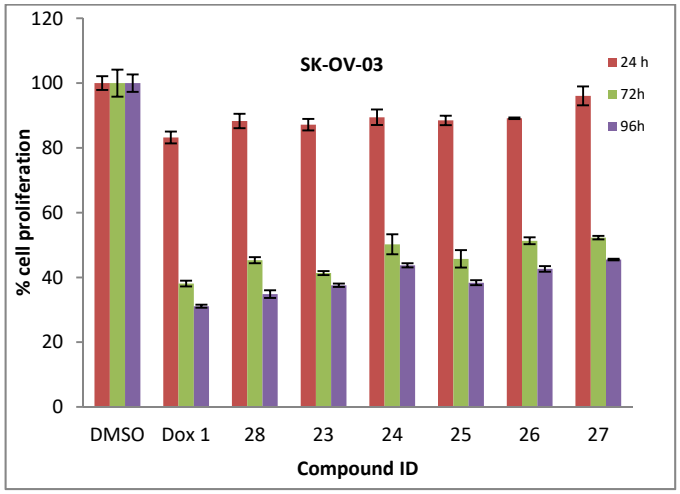

Figure 19. Antiproliferative activity of Dox-acyl derivatives in leukemia (CCRF-CEM) and ovarian (SK-OV-03) cancer cells. Adapted from ref [97] with permission. Copyright ACS.

Similar results have been observed for lipophilic derivatives linked through hydrazone linkage at carbonyl group of Dox.[98] Similarly, the 14-OH derivatization with cholesterol,[99] hyaluronic acid,[100] and other lipophilic groups has shown better *in vitro* and

in vivo pharmacological properties of Dox including reduced cardiotoxicity. The cholesteryl doxorubicin derivatives reported by Choi et al.[99] indicated the similar type of results as observed with fatty acyl derivatives (discussed above). The group synthesized Dox-amine functionalized cholesterol derivatives, which showed the loss in the antiproliferative activity of Dox derivative, indicating and supporting the concept of the requirement of the free amino group of Dox as an important site for its cancer cell inhibition. The introduction of cholesterol via a linker (compound **29** and **30**, Figure 20) at position 14'-OH showed the retention of antiproliferative activity along with showing the improved uptake inside the cells. The overall preliminary results with Dox-cholesterol derivatives are in line with the detailed results observed with Dox-fatty acyl derivatives reported by our group (discussed above).

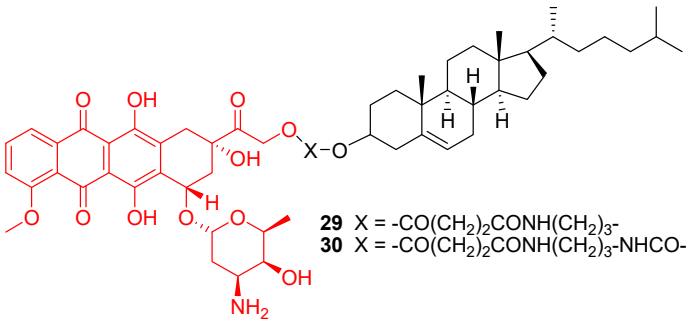

Figure 20. The cholesterol derivatives of Dox reported by Choi et. al.[99]

7. PEPTIDE SYSTEMS

The peptide systems for delivery applications have been preferred molecules of choice due to their natural occurrence, controlled synthesis, and expected higher biocompatibility. Through extensive evaluations, a number of the linear and cyclic peptide havebeen rationalized by different research groups for drug and nucleotide delivery applications.[101] The extensive library of peptides of differing chain lengths and sequences brought the molecular architectural properties of these molecules towards the generation of applicative concepts. The literature on the abundance of the library of novel peptide systems has emerged as a source for designing modular transporters for nuclear drug delivery. Many natural peptide systems have been known to undergo preferred internalization into cells and served the basis for the understanding of the mechanism of their nuclear importation. However, some internalization mechanisms are still unclear and give impetus to designing and synthesis of more variations of peptide structures. This preferential cellular internalization activity of selected peptides (known as Cell Penetrating Peptides (CPP))[102] has been exploited by several research groups for enhancing nuclear drug delivery. Moreover, the peptides have been further conjugated to other delivery systems to improve the target delivery besides having been used as stand-alone to drug delivery applications.[103]

The natural peptide sequences have served the basis for evaluation for application. For example, the TAT-NLS-peptide (YGRKKRRQRRR) **31** (Figure 21) from the HIV-1 TAT protein is known to traverse the nuclear membrane into the nucleoplasm and thus has been conjugated to several drug delivery systems for achieving enhanced delivery.[104] The TAT-peptide is easily recognized by the importin transport receptors IMPα-β1 or IMPβ1 for nuclear entry through the nuclear pore complex (NPCs).

The TAT-peptides conjugated on to mesoporous silica nanoparticles (MSNs-TAT) are able to deliver and release pharmaceutical molecules, such as Dox, into the nucleus.[105] Pan et al. has reported the synthesis of MSNs-TAT nanoparticles with a range of diameters of 25, 50, 67, and 105 nm as obtained by TAT-peptide esterification on the surface of MSNs and further evaluation of nuclear delivery in cervical cancer HeLa cells.[105] Nuclear internalization of nanoparticle peptide conjugate was monitored by conjugating the green fluorescein isothiocyanate FITC on the TAT peptide. The internalization results indicated that after 24h, the MSNs-TAT nanoparticles with a diameter size of 67 and 105 nm did not localize in the nucleus (means could not transport across a nuclear membrane). The large size nanoparticles remained primarily on the nuclear membrane as their larger diameters hindered their entry through the nuclear pore complex NPC. The observation was contrasting with small size nanoparticles. MSNs-TAT nanoparticles with diameter size of 25 and 50 nm entered the nucleus within 4 h. Furthermore, Dox was conjugated on the MSN-TAT nanoparticles, and it was observed that Dox-loadedMSNs-TAT (DOX@MSNs-TAT) nanoconjugate with diameter of 25 nm entered the nuclei of HeLa cells successfully. Comparatively, the free Dox and DOX@MSNs without the TAT-peptide had a negligible transportation across nuclear membrane. These results were supplemented with Transmission electron microscopy (TEM) images which indicated reinforced nuclear entry of 25 and 50 nm MSNs-TAT and no nuclear entry by 67 and 105 nm diameter sized MSNs-TAT. The MSNs nanoparticles of varying sizes without the TAT peptide got internalized into the cytoplasm, but were not found in the nucleoplasm. Conclusively, the MSNs-TAT with a diameter of 50 nm or smaller can efficiently target the nucleus and deliver Dox into the nucleus. This indicates that the TAT peptide served as a crucial nuclear localization signals(NLS) for binding to the importin transport receptors, allowing transport through the nucleoporins of the nuclear pore complex (NPCs).

The nuclear delivery efficiency of TAT peptide has been utilized by many researchers for delivery genes (DNA fragments and siRNA) to the nucleus.[106] TAT-peptide has also been employed in conjunction with other NLS peptides[107] to improve nuclear delivery and has also been utilized with different other nanoparticles.[101]

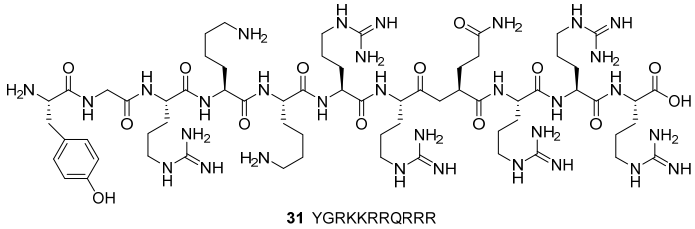

Figure 21. Chemical structure of TAT peptide YGRKKRRQRRR.

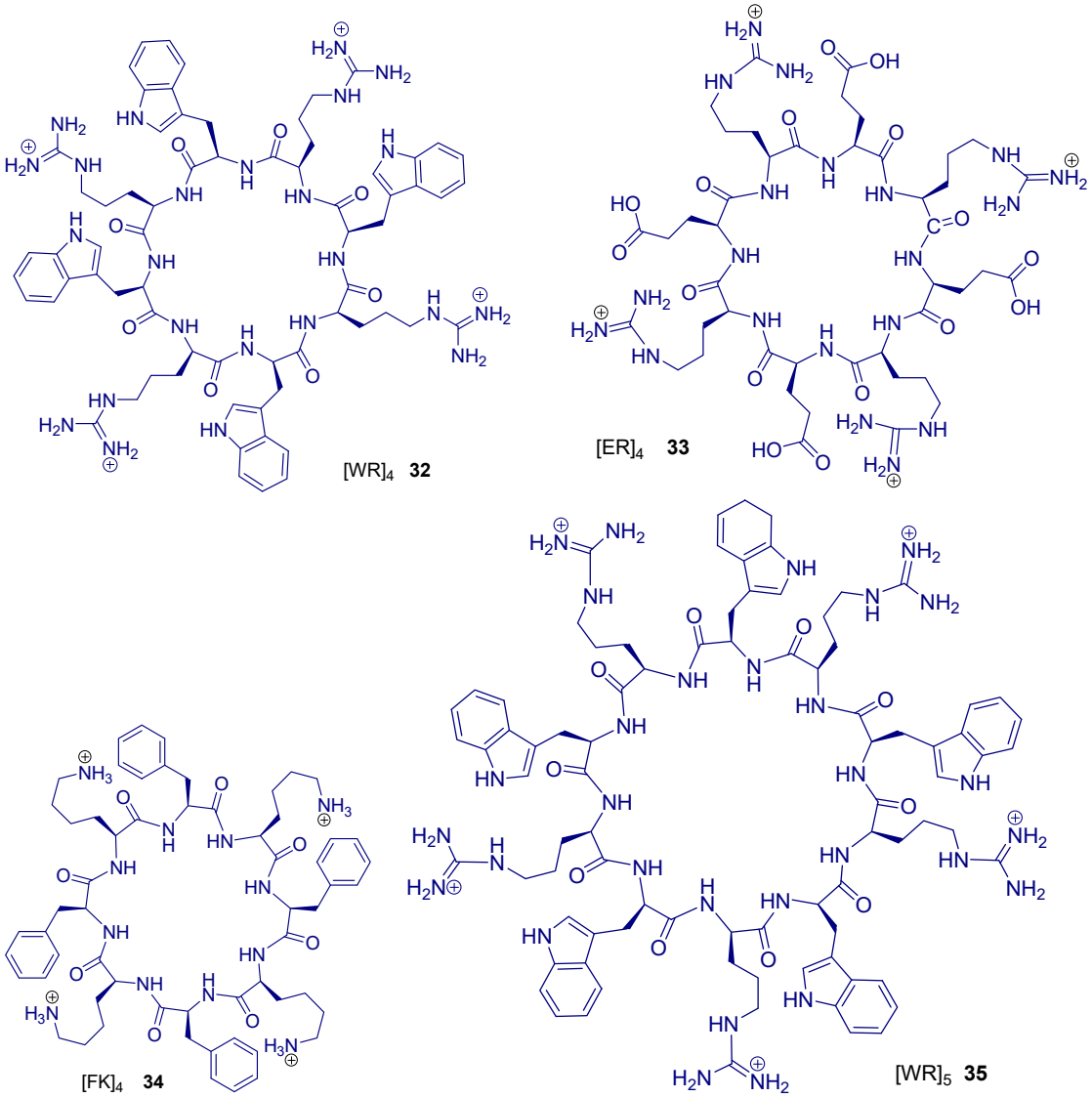

Figure 22. Representative chemical structures of recent examples of cyclic peptides a) [WR]$_4$ **32**b)[ER]$_4$ **33** c)[FK]$_4$ **34**, and d) [WR]$_4$ **35** evaluated for drug delivery applications.

Taking the lead from natural peptides, the designing of peptide for preferential cellular uptake has been an exciting field. The optimum charge balancing using different amino acids (negatively, positively charged and neutral amino acid), variation in charge densities by different sequences of selected amino acids and along with their design architectures (linear and cyclic) as well as length variation of peptides and balanced hydrophilicity-lipophilicity form the fundamental methodology for enhanced interaction with cellular membrane and crossing over through pores. Considering the above conceptual fundamental molecular structure basis of CPPs, we have designed a number of linear and cyclic peptides using Arginine (R) and Tryptophan (W) and other amino acids variations for drug delivery applications (Figure 22)[108] and self-assembling of peptides in nanostructures.[109]

Furthermore, Dox was conjugated to synthesized peptides **36 and 37** (linear as well as cyclic peptides) via its 14'C-OH using a linker between the peptide and the drug, as shown in Figure 23. As the synthesized peptides have preferential uptake in the cancerous cells, the Dox-CPP conjugates accumulated more in the cells. The Dox-CPP conjugate has anti-proliferative profile comparable to free Dox as shown by the Inhibition of leukemia CCRF-CEM, ovarian SK-OV-3, colon HCT-116, and breast MDA-MB-468 cells by CPP-Dox compounds (1 μM) after 24−120 h incubation. The simple mixture of linear (RW)$_4$ peptide + Dox and Cyclic (RW)$_4$ + Dox had similar antiproliferative as that of CPP-Dox conjugates **36** and **37** (Figure 24). This indicates that conjugation of Dox with peptides through 14'C-OH lead to retention of antiproliferative activity of parent Dox, which is in conformity with fatty acyl–Dox conjugate (**23-27**). Further, the fluorescence imaging of cells incubated with free Dox and CPP-Dox **37** showed better accumulation as well as retention of CPP-Dox **37** inside the cells as shown in Figure 25 for imaging after 24 h of incubation. CPP-Dox **37**, thus, showed retention of the therapeutic profile (anti-proliferation activity) with the better uptake and retention for the anti-cancer activity of the Dox drug in different cancer cells, an observation in line with the Dox-fatty acyl derivatives (**23-27**).[110]

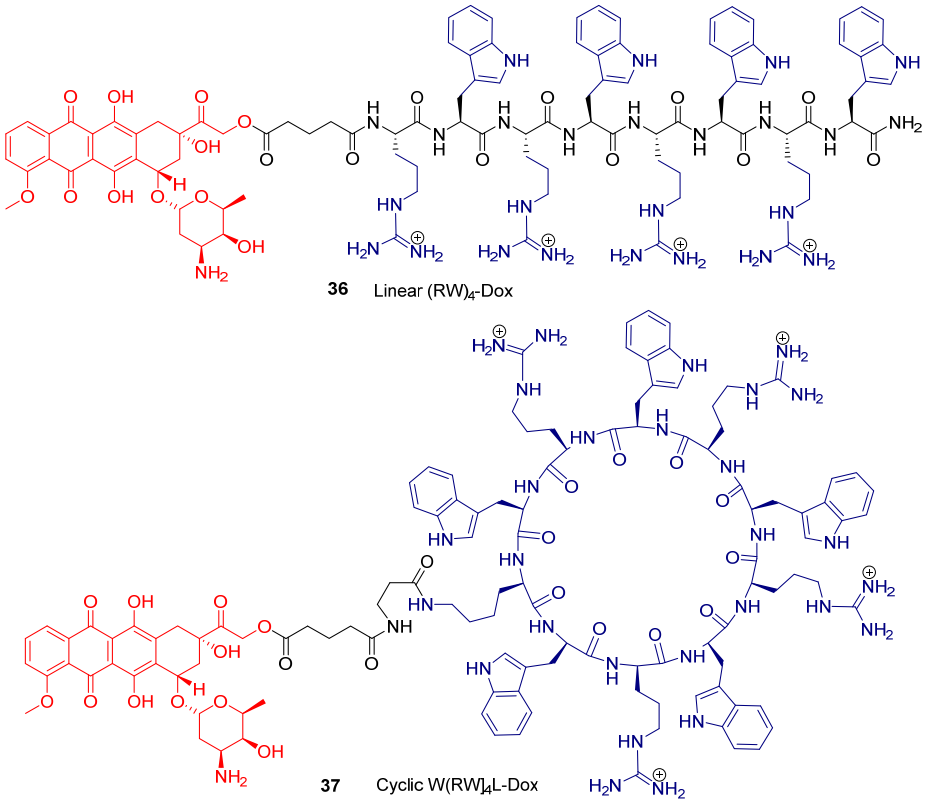

Figure 23. Conjugation of Dox with linear and cyclic Peptides using a linker.

optimal conditions of basic medium to generate Dox-SH, containing an amidine with a free sulfhydryl group. Dox-SH was activated by reacting with pyridyl disulfide (Pyr-SS-Pyr) in acidic medium and obtained the corresponding more reactive Dox-SS-Pyr. This activated Dox-SS-Pyr containing a disulfide bridge permitted the conjugation of Dox with the thiol group in the cysteine of the cyclicpeptide [C(WR)$_4$K] with extrusion of pyridine-2-thione (Figure 26). The CPP-SS-Dox conjugate show comparable anti-proliferative activity as that of Dox at 5 µM concentration.[111] It remains to be determined the type of lysis taking place; whether it is S-S cleavage from conjugate or at the amidine group to release the free Dox inside the cell for activity. In previous case, a reduced or loss of activity would be observed as noted with any functionalization at amine group of Dox.[96]

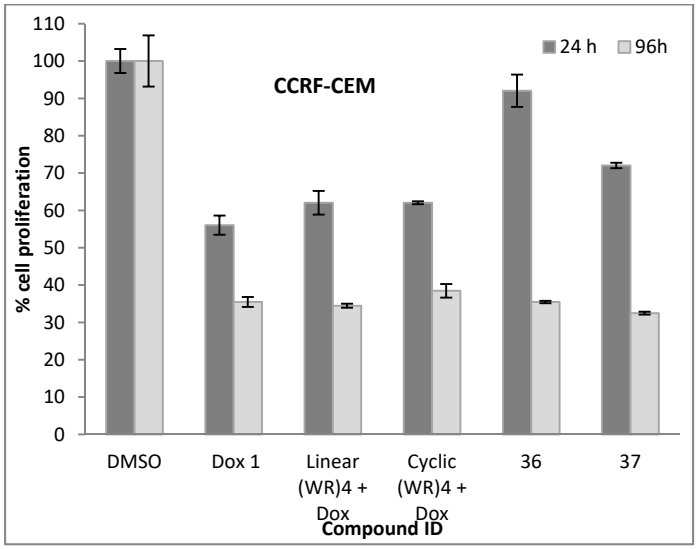

Figure 24. Representative graph for Inhibition of CCRF-CEM cells by control DMSO, free Dox, a mixture of peptides and Dox, and synthesized peptide-Dox conjugates **36, 37** at 1 µM concentration after 24−120 h of incubation. Similar results are shown in SK-OV-3, HCT-116, and MDA-MB-468 as reported by Shirazi et. al.[110] Reproduced with permission. Copyright ACS.

The Dox attachment to CPP [C(WR)$_4$K] via S-S linkage was reported by Darwish et al.[111] The amine group of Dox was reacted with 2-iminothiolane hydrochloride (Traut's reagent) under

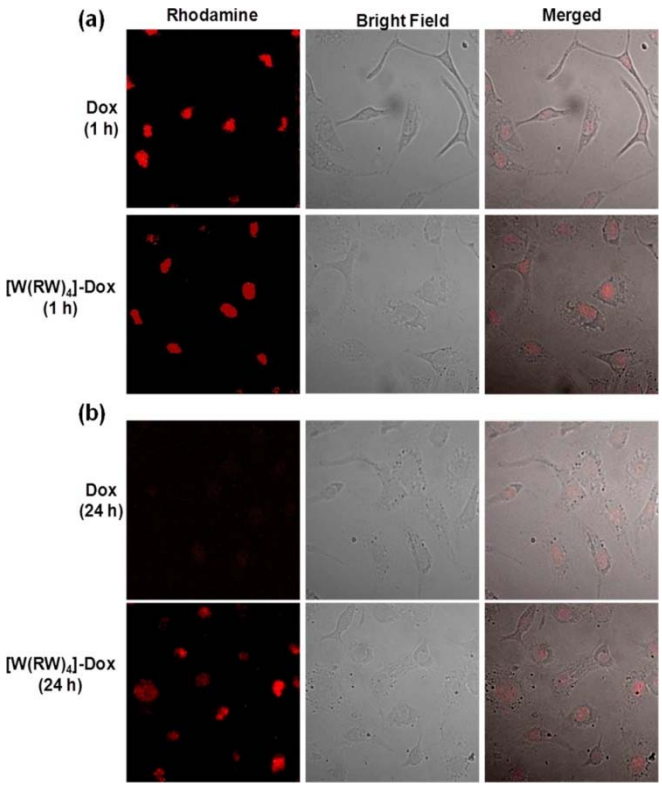

Figure 25. Cellular uptake profile of free Dox and Dox-CPP compound **37** at 1h and 24h as reported by Shirazi et. al.[110] Reproduced with permission. Copyright ACS.

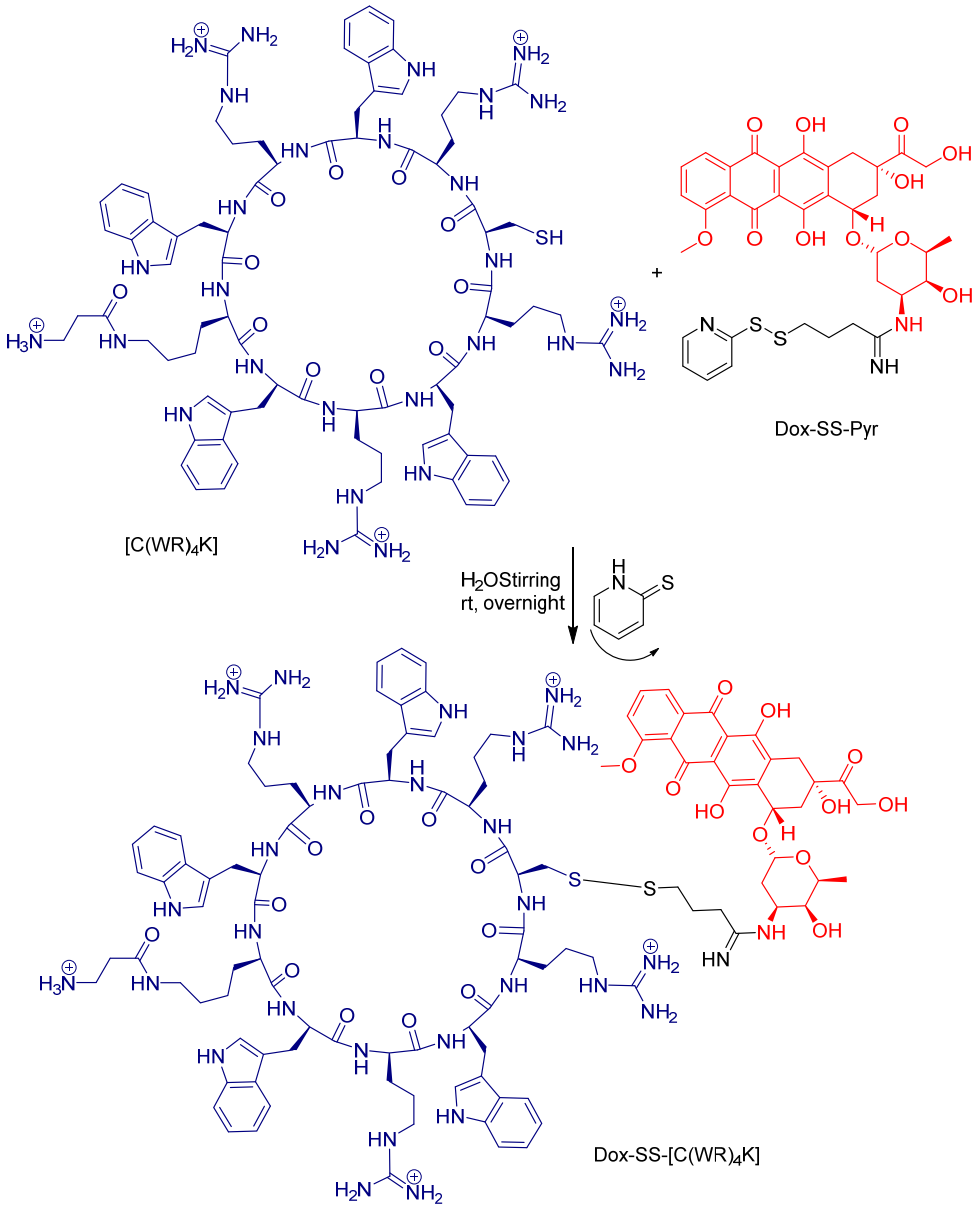

Figure 26. Chemical synthesis of Dox-SS-[C(WR)$_4$K].

he observation of desired pharmacological properties and anti-cancer activity with fatty acyl and peptide conjugates of Dox has opened upon the venue for the exploration of further designed peptides and conjugates having promising clinical applications.

CONCLUSION

In conclusion, the nanoparticulate based (mostly inorganic nanoparticle) delivery systems have not been successful in providing the desired improvement in the delivery and efficacy of Dox. The different nanoparticulate systems posed issues in an amount of drug loading (drug/vehicle ratio) along with reduced release kinetics of drug from nanoconjugate. Many of the reported polymer/lipid-bound or direct nanoparticle-attached Dox release Dox partially. For example, The PEO-TMA-FA coated magnetic nanoparticles system of Maeng et al. released only 56% of total Dox in 24 h at pH 5.1; the PEGylated SPION system of Yang et al. released 35% of Dox after 24 h at pH 5.3 and 40% after more than 75 h; the copolymer coated SPION system of Fang et al. released 55% of Dox in 72 h at pH 5.5; and the PEI-PEGylated system of Kievit et al. released a maximum 30% of Dox at pH range 4.5-7.5. Second, the released kinetics data need to be critically analyzed as any released Dox get adsorbed on dialysis membrane or get precipitated on centrifugation tubes during the experimental analysis. The loss in activity of Dox on conjugation was more prominent for covalent functionalization done using amine group of Dox compared to other functionalizations. The covalently bound Dox attached using amine group usually shows less activity due to the difficultly to get hydrolyze amide linkage. The lipophilic functionalization at 17 OH or carbonyl group with acyl (or alkyl) and cholesterol lipids has produced Dox derivative with desired pharmacological profile as reflected in their *in vitro* and *in vivo* evaluation suggesting for clinical applications. Further developments are warranted to explore the potential delivery tools for Dox.

ACKNOWLEDGMENT

We thank Chapman University School of Pharmacy for the financial Support.

CONFLICT OF INTEREST

Authors declare no conflict of interest.

REFERENCES

1. C.J. Lovitt, T.B. Shelper, V.M. Avery. Doxorubicin resistance in breast cancer cells is mediated by extracellular matrix proteins. *BMC Cancer* **2018**, 18 (1), 41.
2. T. Aas, A.L. Børresen, S. Geisler, et al. Specific P53 mutations are associated with de novo resistance to doxorubicin in breast cancer patients. *Nat. Med.* **1996**, 2 (7), 811–814.
3. Y. Tang, A.J. McGoron, T. Y., M. A.J. Combined effects of laser-ICG photothermotherapy and doxorubicin chemotherapy on ovarian cancer cells. *J. Photochem. Photobiol. B Biol.* **2009**, 97 (3), 138–144.
4. R.P. Bandari, M.R. Lewis, C.J. Smith. Synthesis and Evaluation of [DUPA-6-Ahx-Lys (DOTA)-6-Ahx-RM2], a Novel, Bivalent Targeting Ligand for GRPr/PSMA Biomarkers of Prostate Cancer. *Chem. Biol. Lett.* **2018**, 5 (1), 11–24.
5. A.K. Mittal, K. Thanki, S. Jain, U.C. Banerjee. Comparative studies of anticancer and antimicrobial potential of bioinspired silver and silver-selenium nanoparticles. *J. Mater. Nanosci.* **2016**, 3 (1), 22–27.

6. D.P. de Lima, T.N. Reddy, A. Beatriz, et al. Design, synthesis and Structure-Activity Relationship of novel Phenolic based Pyrimidine hybrids from Cashew Nut Shell Liquid (CNSL) components as potential antitumor agents. *Chem. Biol. Lett.* **2018**, 5 (2), 41–54.
7. C. Riganti, C. Voena, J. Kopecka, et al. Liposome-Encapsulated Dox Reverses Drug Resistance by Inhibiting P-Glycoprotein in Human Cancer Cells. *Mol. Pharm.* **2011**, 8 (3), 683–700.
8. C. Carvalho, R. Santos, S. Cardoso, et al. Doxorubicin: The Good, the Bad and the Ugly Effect. *Curr. Med. Chem.* **2009**, 16 (25), 3267–3285.
9. K. Chatterjee, J. Zhang, N. Honbo, J.S. Karliner. Doxorubicin cardiomyopathy. *Cardiology* **2010**, 115 (2), 155–162.
10. S.A. Abraham, D.N. Waterhouse, L.D. Mayer, et al. The liposomal formulation of doxorubicin. *Methods Enzymol.* **2005**, 391 (SPEC. ISS.), 71–97.
11. J. Singh, B.S. Chhikara. Comparative global epidemiology of HIV infections and status of current progress in treatment. *Chem. Biol. Lett.* **2014**, 1 (1), 14–32.
12. Y.C. Barenholz. Doxil®—the first FDA-approved nano-drug: lessons learned. *J. Control. Release* **2012**, 160 (2), 117–134.
13. T. Safra, F. Muggia, S. Jeffers, et al. Pegylated liposomal doxorubicin (doxil): reduced clinical cardiotoxicity in patients reaching or exceeding cumulative doses of 500 mg/m2. *Ann. Oncol.* **2000**, 11 (8), 1029–1033.
14. C. Sanson, C. Schatz, J.-F.F. Le Meins, et al. A simple method to achieve high doxorubicin loading in biodegradable polymersomes. *J. Control. Release* **2010**, 147 (3), 428–435.
15. K. Deepa, S. Singha, T. Panda. Doxorubicin Nanoconjugates. *J. Nanosci. Nanotechnol.* **2014**, 14 (1), 892–904.
16. J. Singh, S. Kumar, B. Rathi, K. Bhrara, B.S. Chhikara. Therapeutic analysis of Terminalia arjuna plant extracts in combinations with different metal nanoparticles. *J. Mater. Nanosci.* **2015**, 2 (1), 1–7.
17. S.S. Malapure, S. Bhushan, R. Kumar, S. Bharati. Radiolabelled nanoparticles in cancer management: current status and developments. *Chem. Biol. Lett.* **2018**, 5 (1), 25–34.
18. J. Gautier, E. Allard-Vannier, E. Munnier, M. Soucé, I. Chourpa. Recent advances in theranostic nanocarriers of doxorubicin based on iron oxide and gold nanoparticles. *J. Control. Release* **2013**, 169 (1–2), 48–61.
19. J. You, G.D. Zhang, C. Li. Exceptionally High Payload of Doxorubicin in Hollow Gold Nanospheres for Near-Infrared Light-Triggered Drug Release. In *ACS Nano*; **2010**; Vol. 4, pp 1033–1041.
20. J.H. Maeng, D.-H.H. Lee, K.H. Jung, et al. Multifunctional doxorubicin loaded superparamagnetic iron oxide nanoparticles for chemotherapy and magnetic resonance imaging in liver cancer. *Biomaterials* **2010**, 31 (18), 4995–5006.
21. K. Min, H. Jo, K. Song, et al. Dual-aptamer-based delivery vehicle of doxorubicin to both PSMA (+) and PSMA (-) prostate cancers. *Biomaterials* **2011**, 32 (8), 2124–2132.
22. X. He, X. Wu, X. Cai, et al. Functionalization of magnetic nanoparticles with dendritic–linear–brush-like triblock copolymers and their drug release properties. *Langmuir* **2012**, 28 (32), 11929–11938.
23. H.-M.M. Yang, B.C. Oh, J.-D.H.D. Kim, et al. Multifunctional poly (aspartic acid) nanoparticles containing iron oxide nanocrystals and doxorubicin for simultaneous cancer diagnosis and therapy. *Colloids Surfaces A Physicochem. Eng. Asp.* **2011**, 391 (1–3), 208–215.
24. Q. Quan, J. Xie, H. Gao, et al. HSA coated iron oxide nanoparticles as drug delivery vehicles for cancer therapy. *Mol. Pharm.* **2011**, 8 (5), 1669–1676.
25. S. Park, H.S. Kim, W.J. Kim, H.S. Yoo. Pluronic @ Fe 3 O 4 nanoparticles with robust incorporation of doxorubicin by. *International Journal of Pharmaceutics*. 2012, pp 107–114.
26. D. Silvestri, S. Wacławek, B. Sobel, et al. A poly(3-hydroxybutyrate)–chitosan polymer conjugate for the synthesis of safer gold nanoparticles and their applications. *Green Chem.* **2018**, 20 (21), 4975–4982.
27. P. Moitra, K. Kumar, S. Sarkar, et al. New pH-responsive gemini lipid derived co-liposomes for efficacious doxorubicin delivery to drug resistant cancer cells. *Chem. Commun.* **2017**, 53 (58), 8184–8187.
28. Y.-J. Gu, J. Cheng, C.W.-Y. Man, W.-T. Wong, S.H. Cheng. Gold-doxorubicin nanoconjugates for overcoming multidrug resistance. *Nanomedicine Nanotechnology, Biol. Med.* **2012**, 8 (2), 204–211.
29. M. Prabaharan, J.J. Grailer, S. Pilla, D.A. Steeber, S. Gong. Gold nanoparticles with a monolayer of doxorubicin-conjugated amphiphilic block copolymer for tumor-targeted drug delivery. *Biomaterials* **2009**, 30 (30), 6065–6075.
30. S. Aryal, J.J. Grailer, S. Pilla, et al. Doxorubicin conjugated gold nanoparticles as water-soluble and pH-responsive anticancer drug nanocarriers. *J. Mater. Chem.* **2009**, 19 (42), 7879–7884.
31. F. Wang, Y.-C. Wang, S. Dou, et al. Doxorubicin-Tethered Responsive Gold Nanoparticles Facilitate Intracellular Drug Delivery for Overcoming Multidrug Resistance in Cancer Cells. *ACS Nano* **2011**, 5 (5), 3679–3692.
32. A.Z. Mirza, H. Shamshad. Preparation and characterization of doxorubicin functionalized gold nanoparticles. *Eur. J. Med. Chem.* **2011**, 46 (5), 1857–1860.
33. O.A. Swiech, L.J. Opuchlik, G. Wojciuk, et al. Doxorubicin carriers based on Au nanoparticles-effect of shape and gold-drug linker on the carrier toxicity and therapeutic performance. *RSC Adv.* **2016**, 6 (38).
34. Y. Du, L. Xia, A. Jo, et al. Synthesis and Evaluation of Doxorubicin-Loaded Gold Nanoparticles for Tumor-Targeted Drug Delivery. *Bioconjug. Chem.* **2018**, 29 (2), 420–430.
35. L. Lacroix, A. Meffre, C. Gatel, et al. Nanoparticle Ripening : A Versatile Approach for the Size and Shape Control of Metallic Iron Nanoparticles. *Chempluschem* **2019**, 84 (3), 302–306.
36. M.-Y. Hua, H.-W. Yang, H.-L. Liu, et al. Superhigh-magnetization nanocarrier as a doxorubicin delivery platform for magnetic targeting therapy. *Biomaterials* **2011**, 32 (34), 8999–9010.
37. P. Kumar, G. Behl, M. Sikka, A. Chhikara, M. Chopra. Poly(ethylene glycol)-co-methacrylamide-co-acrylic acid based nanogels for delivery of doxorubicin. *J. Biomater. Sci. Polym. Ed.* **2016**, 27 (14), 1413–1433.
38. C. Fang, F.M. Kievit, O. Veiseh, et al. Fabrication of magnetic nanoparticles with controllable drug loading and release through a simple assembly approach. *J. Control. Release* **2012**, 162 (1), 233–241.
39. F.M. Kievit, F.Y. Wang, C. Fang, et al. ox loaded iron oxide nanoparticles overcome multidrug resistance in cancer in vitro. *J. Control. Release* **2011**, 152 (1), 76–83.
40. J. Ma, X. Lü, Y. Huang. Genomic analysis of cytotoxicity response to nanosilver in human dermal fibroblasts. *J. Biomed. Nanotechnol.* **2011**, 7 (2), 263–275.
41. A. Hekmat, A.A. Saboury, A. Divsalar. The effects of silver nanoparticles and doxorubicin combination on DNA structure and its antiproliferative effect against T47D and MCF7 cell lines. *J. Biomed. Nanotechnol.* **2012**, 8 (6), 968–982.
42. F. Ravaux, J.-C.J.-C. Olsen, M. Magzoub, et al. Synthesis of silver nanoparticles for the dual delivery of doxorubicin and alendronate to cancer cells. *J. Mater. Chem. B* **2015**, 3 (36), 7237–7245.
43. J. Encarnación-Rosado, K. Habiba, K. García-Pabón, B.R. Weiner, G. Morell. Abstract 2196: Improving cytotoxicity against cancer cells by chemo-photodynamics combined modalities using silver/graphene quantum dots/doxorubicin nanoconjugates. *Cancer Res.* **2016**, 76 (14), 2196–2196.
44. J. Shi, L. Wang, J. Zhang, et al. A tumor-targeting near-infrared laser-triggered drug delivery system based on GO@Ag nanoparticles for chemo-photothermal therapy and X-ray imaging. *Biomaterials* **2014**, 35 (22), 5847–5861.
45. P. Kumari, R. Gautam, A. Milhotra. Application of Porphyrin nanomaterials in Photodynamic therapy. *Chem. Biol. Lett.* **2016**, 3 (2), 32–37.
46. L. Qi, X. Gao. Emerging application of quantum dots for drug delivery and therapy. *Expert Opin. Drug Deliv.* **2008**, 5 (3), 263–267.
47. P.M. Chaudhary, R.V. Murthy, R. Kikkeri. Advances and prospects of sugar capped Quantum Dots. *J. Mater. Nanosci.* **2014**, 1 (1), 7–11.
48. J.B. Delehanty, K. Boeneman, C.E. Bradburne, K. Robertson, I.L. Medintz. Quantum dots: a powerful tool for understanding the intricacies of nanoparticle-mediated drug delivery. *Expert Opin. Drug Deliv.* **2009**, 6 (10), 1091–1112.
49. V. Bagalkot, L. Zhang, E. Levy-Nissenbaum, et al. Quantum dot-aptamer conjugates for synchronous cancer imaging, therapy, and sensing of drug delivery based on Bi-fluorescence resonance energy transfer. *Nano Lett.* **2007**, 7 (10), 3065–3070.

50. R. Savla, O. Taratula, O. Garbuzenko, T. Minko. Tumor targeted quantum dot-mucin 1 aptamer-doxorubicin conjugate for imaging and treatment of cancer. *J. Control. Release* **2011**, 153 (1), 16–22.
51. D. Jhanwar, J. Sharma. Chemotherapeutic and chemopreventive effect of ZnO nanoparticles on DMBA/croton oil induced mice skin carcinogenesis. *J. Mater. Nanosci.* **2016**, 3 (1), 28–32.
52. Q. Chen, P. Wang, P.S. Low, S.A. Kularatne. Recent advances in PET imaging of folate receptor positive diseases. *Chem. Biol. Lett.* **2014**, 1 (2), 55–65.
53. F. Muhammad, M. Guo, Y. Guo, et al. Acid degradable ZnO quantum dots as a platform for targeted delivery of an anticancer drug. *J. Mater. Chem.* **2011**, 21 (35), 13406–13412.
54. X. Cai, Y. Luo, W. Zhang, D. Du, Y. Lin. PH-Sensitive ZnO Quantum Dots-Doxorubicin Nanoparticles for Lung Cancer Targeted Drug Delivery. *ACS Appl. Mater. Interfaces* **2016**, 8 (34), 22442–22450.
55. S.K. Tripathi, G. Kaur, R.K. Khurana, S. Kapoor, B. Singh. Quantum Dots and their Potential Role in Cancer Theranostics. *Crit. Rev. Ther. Drug Carrier Syst.* **2015**, 32 (6), 461–502.
56. J. Encarnación-Rosado, K. Habiba, K. García-Pabón, et al. Clinical potential of quantum dots. *Acta Biomater.* **2013**, 88 (12), 443–447.
57. N. Durán, M.B. Simões, A.C.M. De Moraes, W.J. Fávaro, A.B. Seabra. Nanobiotechnology of carbon dots: A review. *J. Biomed. Nanotechnol.* **2016**, 12 (7), 1323–1347.
58. M. Alibolandi, K. Abnous, F. Sadeghi, et al. Folate receptor-targeted multimodal polymersomes for delivery of quantum dots and doxorubicin to breast adenocarcinoma: In vitro and in vivo evaluation. *Int. J. Pharm.* **2016**, 500 (1–2), 162–178.
59. R. Hu, H. Zheng, J. Cao, Z. Davoudi, Q. Wang. Synthesis and *In Vitro* Characterization of Carboxymethyl Chitosan-CBA-Doxorubicin Conjugate Nanoparticles as pH-Sensitive Drug Delivery Systems. *J. Biomed. Nanotechnol.* **2017**, 13 (9), 1097–1105.
60. H. Dong, C. Dong, T. Ren, D. Shi. Surface-engineered graphene-based nanomaterials for drug delivery. *J. Biomed. Nanotechnol.* **2014**, 10 (9), 2086–2106.
61. J. Shen, Q. He, Y. Gao, J. Shi, Y. Li. Mesoporous silica nanoparticles loading doxorubicin reverse multidrug resistance: Performance and mechanism. *Nanoscale* **2011**, 3 (10), 4314–4322.
62. Y. Gao, Y. Chen, X. Ji, et al. Controlled Intracellular Release of Doxorubicin in Multidrug-Resistant Cancer Cells by Tuning the Shell-Pore Sizes of Mesoporous Silica Nanoparticles. *ACS Nano* **2011**, 5 (12), 9788–9798.
63. H. Meng, M. Liong, T. Xia, et al. Engineered Design of Mesoporous Silica Nanoparticles to Deliver Doxorubicin and P-Glycoprotein siRNA to Overcome Drug Resistance in a Cancer Cell Line. *ACS Nano* **2010**, 4 (8), 4539–4550.
64. X. Hu, X. Hao, Y. Wu, et al. Multifunctional hybrid silica nanoparticles for controlled doxorubicin loading and release with thermal and pH dual response. *J. Mater. Chem. B* **2013**, 1 (8), 1109–1118.
65. Q. Zhang, D. Li, H. Zhao, S. Du, L. Liu. A surface-grafted ligand functionalization strategy for coordinate binding of doxorubicin at surface of PEGylated mesoporous silica nanoparticles: Toward pH-responsive drug delivery. *Colloids Surfaces B Biointerfaces* **2017**, 149, 138–145.
66. X. Wang, C. Li, N. Fan, et al. Multimodal nanoporous silica nanoparticles functionalized with aminopropyl groups for improving loading and controlled release of doxorubicin hydrochloride. *Mater. Sci. Eng. C* **2017**, 78, 370–375.
67. R.C.H. Wong, D.K.P. Ng, W.-P. Fong, P.-C. Lo. Encapsulating pH-Responsive Doxorubicin-Phthalocyanine Conjugates in Mesoporous Silica Nanoparticles for Combined Photodynamic Therapy and Controlled Chemotherapy. *Chem. - A Eur. J.* **2017**, 23 (65), 16505–16515.
68. A. Pal, B.S. Chhikara, A. Govindaraj, S. Bhattacharya, C.N.R. Rao. Synthesis and properties of novel nanocomposites made of single-walled carbon nanotubes and low molecular mass organogels and their thermo-responsive behavior triggered by near IR radiation. *J. Mater. Chem.* **2008**, 18 (22), 2593–2600.
69. S.K. Misra, P. Moitra, B.S. Chhikara, P. Kondaiah, S. Bhattacharya. Loading of single-walled carbon nanotubes in cationic cholesterol suspensions significantly improves gene transfection efficiency in serum. *J. Mater. Chem.* **2012**, 22 (16), 7985–7998.
70. B.S. Chhikara, S.K. Misra, S. Bhattacharya. CNT loading into cationic cholesterol suspensions show improved DNA binding and serum stability and ability to internalize into cancer cells. *Nanotechnology* **2012**, 23 (6), 65101.
71. Z. Liu, A.C. Fan, K. Rakhra, et al. Supramolecular Stacking of Doxorubicin on Carbon Nanotubes for In Vivo Cancer Therapy. *Angew. Chemie Int. Ed.* **2009**, 48 (41), 7668–7672.
72. L. Meng, X. Zhang, Q. Lu, Z. Fei, P.J. Dyson. Single walled carbon nanotubes as drug delivery vehicles: Targeting doxorubicin to tumors. *Biomaterials* **2012**, 33 (6), 1689–1698.
73. C.M.Q. Le, X.T. Cao, D.W. Kim, et al. Preparation of poly(styrene- *alt* -maleic anhydride) grafted multi-walled carbon nanotubes for pH-responsive release of doxorubicin. *Mol. Cryst. Liq. Cryst.* **2017**, 654 (1), 181–189.
74. P. Chaudhuri, A. Paraskar, S. Soni, R.A. Mashelkar, S. Sengupta. Fullerenol-cytotoxic conjugates for cancer chemotherapy. *ACS Nano* **2009**, 3 (9), 2505–2514.
75. L. Zhao, H. Li, L. Tan. A Novel Fullerene-Based Drug Delivery System Delivering Doxorubicin for Potential Lung Cancer Therapy. *J. Nanosci. Nanotechnol.* **2017**, 17 (8), 5147–5154.
76. A.J. Pollard, N. Kumar, A. Rae, et al. Nanoscale Optical Spectroscopy: An Emerging Tool for the Characterisation of 2 D Materials. *J. Mater. Nanosci.* **2014**, 1 (1), 39–49.
77. C.N.R. Rao, A.K. Sood, K.S. Subrahmanyam, A. Govindaraj. Graphene: The new two-dimensional nanomaterial. *Angew. Chemie - Int. Ed.* **2009**, 48 (42), 7752–7777.
78. A.M. Pinto, I.C. Gonçalves, F.D. Magalhães. Graphene-based materials biocompatibility: A review. *Colloids Surfaces B Biointerfaces* **2013**, 111, 188–202.
79. B.S. Chhikara, R.S. Varma. Nanochemistry and Nanocatalysis Science: Research advances and future perspectives. *J. Mater. Nanosci.* **2019**, 6 (1), 1–6.
80. B.S. Chhikara. Current trends in nanomedicine and nanobiotechnology research. *J. Mater. Nanosci.* **2017**, 4 (1), 19–24.
81. B.S. Chhikara. Prospects of Applied Nanomedicine. *J. Mater. Nanosci.* **2016**, 3 (1), 20–21.
82. X. Sun, Z. Liu, K. Welsher, et al. Nano-graphene oxide for cellular imaging and drug delivery. *Nano Res.* **2008**, 1 (3), 203–212.
83. W. Liang, Y. Huang, D. Lu, et al. β-Cyclodextrin–Hyaluronic Acid Polymer Functionalized Magnetic Graphene Oxide Nanocomposites for Targeted Photo-Chemotherapy of Tumor Cells. *Polymers (Basel).* **2019**, 11 (1), 133.
84. S. Shen, C. Cui, Z. Guo, et al. PEGylated doxorubicin cloaked nano-graphene oxide for dual-responsive photochemical therapy. *Int. J. Pharm.* **2019**, 557 (September 2018), 66–73.
85. S. Mousa, D. Bharali, M. Khalil, M. Gurbuz, Simone. Nanoparticles and cancer therapy: A concise review with emphasis on dendrimers. *Int. J. Nanomedicine* **2010**, 1.
86. O.L. Padilla De Jesus, H.R. Ihre, L. Gagne, et al. Polyester dendritic systems for drug delivery applications: in vitro and in vivo evaluation. *Bioconjug Chem* **2002**, 13 (3), 453–461.
87. P.S. Lai, P.J. Lou, C.L. Peng, et al. Doxorubicin delivery by polyamidoamine dendrimer conjugation and photochemical internalization for cancer therapy. *J Control Release* **2007**, 122 (1), 39–46.
88. B.S. Chhikara, D. Mandal, K. Parang. Synthesis and evaluation of fatty acyl ester derivatives of cytarabine as anti-leukemia agents. *Eur. J. Med. Chem.* **2010**, 45 (10), 4601–4608.
89. B.S. Chhikara, K. Parang. Development of cytarabine prodrugs and delivery systems for leukemia treatment. *Expert Opin. Drug Deliv.* **2010**, 7 (12), 1399–1414.
90. B.S. Chhikara, R. Tiwari, K. Parang. N-Myristoylglutamic Acid Derivative of 3'-Fluoro-3'-Deoxythymidine as an Organogel. *Tetrahedron Lett.* **2012**, 53 (39), 5335–5337.
91. H.K. Agarwal, K.W. Buckheit, R.W. Buckheit, K. Parang. Synthesis and anti-HIV activities of symmetrical dicarboxylate esters of dinucleoside

reverse transcriptase inhibitors. *Bioorganic Med. Chem. Lett.* **2012**, 22 (17), 5451–5454.
92. H.K. Agarwal, B.S. Chhikara, M. Quiterio, G.F. Doncel, K. Parang. Synthesis and anti-HIV activities of glutamate and peptide conjugates of nucleoside reverse transcriptase inhibitors. *J Med Chem* **2012**, 55 (6), 2672–2687.
93. H.K. Agarwal, B.S. Chhikara, M.J. Hanley, et al. Synthesis and biological evaluation of fatty acyl ester derivatives of (-)-2′,3′-dideoxy-3′-thiacytidine. *J. Med. Chem.* **2012**, 55 (10), 4861–4871.
94. H.K. Agarwal, B.S. Chhikara, S. Bhavaraju, et al. Emtricitabine prodrugs with improved anti-hiv activity and cellular uptake. *Mol. Pharm.* **2013**, 10 (2), 467–476.
95. H.K. Agarwal, B.S. Chhikara, G.F. Doncel, K. Parang. Synthesis and anti-HIV activities of unsymmetrical long chain dicarboxylate esters of dinucleoside reverse transcriptase inhibitors. *Bioorganic Med. Chem. Lett.* **2017**, 27 (9), 1934–1937.
96. B.S. Chhikara, N. St. Jean, D. Mandal, A. Kumar, K. Parang. Fatty acyl amide derivatives of doxorubicin: Synthesis and in vitro anticancer activities. *Eur. J. Med. Chem.* **2011**, 46 (6), 2037–2042.
97. B.S. Chhikara, D. Mandal, K. Parang. Synthesis, anticancer activities, and cellular uptake studies of lipophilic derivatives of doxorubicin succinate. *J. Med. Chem.* **2012**, 55 (4), 1500–1510.
98. K. F. DOXO-EMCH (INNO-206): The first albumin-binding prodrug of doxorubicin to enter clinical trials. *Expert Opin. Investig. Drugs* **2007**, 16 (6), 855–866.
99. J.S. Choi, K.O. Doh, B.K. Kim, Y.B. Seu. Synthesis of cholesteryl doxorubicin and its anti-cancer activity. *Bioorganic Med. Chem. Lett.* **2017**, 27 (4), 723–728.
100. J. Liao, H. Zheng, Z. Fei, et al. Tumor-targeting and pH-responsive nanoparticles from hyaluronic acid for the enhanced delivery of doxorubicin. *Int. J. Biol. Macromol.* **2018**, 113, 737–747.
101. F. Araste, K. Abnous, M. Hashemi, et al. Peptide-based targeted therapeutics: Focus on cancer treatment. *J. Control. Release* **2018**, 292, 141–162.
102. M. Lindgren, M. Hällbrink, A. Prochiantz, Ü. Langel. Cell-penetrating peptides. *Trends in Pharmacological Sciences*. Elsevier Current Trends March 1, 2000, pp 99–103.
103. M.E. Martin, K.G. Rice. Peptide-guided gene delivery. *AAPS J.* **2007**, 9 (1), E18–E29.
104. H. Brooks, B. Lebleu, E. Vivès. Tat peptide-mediated cellular delivery: Back to basics. *Adv. Drug Deliv. Rev.* **2005**, 57 (4), 559–577.
105. L. Pan, Q. He, J. Liu, et al. Nuclear-Targeted Drug Delivery of TAT Peptide-Conjugated Monodisperse Mesoporous Silica Nanoparticles. *J. Am. Chem. Soc.* **2012**, 134 (13), 5722–5725.
106. Y. Zhou, G. Quan, Q. Wu, et al. Mesoporous silica nanoparticles for drug and gene delivery. *Acta Pharm. Sin. B* **2018**, 8 (2), 165–177.
107. V. Escriou, M. Carrière, D. Scherman, P. Wils. NLS bioconjugates for targeting therapeutic genes to the nucleus. *Adv. Drug Deliv. Rev.* **2003**, 55 (2), 295–306.
108. D. Mandal, A. Nasrolahi Shirazi, K. Parang. Cell-Penetrating Homochiral Cyclic Peptides as Nuclear-Targeting Molecular Transporters. *Angew. Chemie Int. Ed.* **2011**, 50 (41), 9633–9637.
109. D. Mandal, A. Nasrolahi Shirazi, K. Parang. Self-assembly of peptides to nanostructures. *Org. Biomol. Chem.* **2014**, 12 (22), 3544–3561.
110. A. Nasrolahi Shirazi, R. Tiwari, B.S. Chhikara, D. Mandal, K. Parang. Design and biological evaluation of cell-penetrating peptide-doxorubicin conjugates as prodrugs. *Mol. Pharm.* **2013**, 10 (2), 488–499.
111. S. Darwish, N. Sadeghiani, S. Fong, et al. Synthesis and antiproliferative activities of doxorubicin thiol conjugates and doxorubicin-SS-cyclic peptide. *Eur. J. Med. Chem.* **2019**, 161, 594–606.

AUTHORS BIOGRAPHIES

Dr. BS Chhikara is a medicinal organic chemistry researcher with Ph.D. in Biomedical Sciences from University of Delhi and Institute of Nuclear Medicine and Allied Science (DRDO), New Delhi. He did his postdoctoral research at Indian Institute of Science, Bangalore, India (with Prof. Santanu Bhattacharya) and University of Rhode Island, Kingston, RI, USA (with Prof. Keykavous Parang). He has wide research experience in field of radiopharmaceuticals, organic synthesis, medicinal chemistry, catalysis, green chemistry, nanomedicine of carbon nanotubes and lipids, gene delivery, anti-cancer and anti-HIV drugs development. He is associated as Editor of Chemical Biology Letters journal. He has authored 3 books and 45 peer-reviewed articles in international journals.

Dr. Brijesh Rathi, an Assistant Professor of Chemistry at Hansraj College, University of Delhi, completed his doctoral degree in Chemistry from University of Delhi in 2010. Dr. Rathi was a Visiting Assistant Professor (2016-2017) at Department of Chemistry, Massachusetts Institute of Technology (MIT), Cambridge, USA. He holds the position of Section Editor and Associate Editor for Current Topics in Medicinal Chemistry and Chemical Biology Letters, respectively. He is a recipient of prestigious Young Scientist Fellowship, Early Career Research Award and UGC-Raman International Fellowship from Government of India. He was awarded esteemed "Excellence Awards for In Service Teachers - 2018" by University of Delhi. His research includes the discovery of new chemical libraries as antimalarial therapeutics, analysis of structure-activity relationship, and development of the lead molecules aided with hit to lead approach. In last few years, his group has identified several novel promising molecules with potent antiplasmodial activity. Successive synthetic and biological strategies have resulted in discovery of few hits with multistage activity. He has published more than 42 papers in various journals of National and International repute.

Dr. Parang is Associate Dean of Research, Graduate Studies, and Global Affairs and a Full Professor of Medicinal Chemistry and Pharmacology at Chapman University School of Pharmacy in Irvine, California and a member of Chao Family Comprehensive Cancer Center, at University of California, Irvine. He earned a Pharm.D. degree from Tehran University of Medical Sciences in 1989. He received his Ph.D. in medicinal chemistry from the Faculty of Pharmacy at the University of Alberta in 1997, followed by a postdoctoral study in the field solid-phase organic synthesis in Department of Chemistry. He pursued additional postdoctoral studies at Rockefeller University in New York and Johns Hopkins University in Baltimore in bioorganic chemistry. He joined the University of Rhode Island in October 2000 and became a full professor in July 2008. He served as the Program Coordinator of Rhode Island IDeA Network of Biomedical Research Excellence (RI-INBRE) NIH program (2012-2013). He joined Chapman University to assist in establishing School of Pharmacy. He is an author of 188 peer- reviewed publications, 10 patents, and 171 meeting abstracts.